

1 **DNA methylation dynamics during stress-response in woodland strawberry (*Fragaria***
2 ***vesca*)**

3
4 María-Estefanía López^{1,2}, David Roquis¹, Claude Becker³, Béatrice Denoyes⁴ and Etienne
5 Bucher^{1*}

6
7 ¹Crop Genome Dynamics Group, Agroscope, 1260 Nyon, Switzerland, ²Department of Botany
8 and Plant Biology, Faculty of Sciences, University of Geneva, Geneva, Switzerland, ³LMU
9 BioCenter, Faculty of Biology, Ludwig-Maximilians-University Munich, D-82152 Martinsried,
10 Germany and ⁴Univ. Bordeaux, INRAE, Biologie du Fruit et Pathologie, F-33140 Villenave
11 d’Ornon, France

12
13 Correspondance:

14
15 Etienne Bucher
16 E-mail: etienne.bucher@agroscope.admin.ch
17 Tél. : +41 58 483 97 53
18 Mobile : +41 79 158 54 65

19
20 María-Estefanía López (ORCID ID: 0000-0001-9068-4909)
21 David Roquis (ORCID ID: 0000-0001-5265-3132)
22 Claude Becker (ORCID ID: 0000-0003-3406-4670)
23 Béatrice Denoyes (ORCID ID: 0000-0002-0369-9609)
24 Etienne Bucher (ORCID ID: 0000-0002-3114-3763)
25

Total word count (excluding summary, references, and legends)	6479	No. of figures:	7 (all in color)
Summary:	199	No. of Tables:	1
Introduction:	804	No. of Supporting Information files:	11 (Fig. S1- S4; Table S1-S7)
Materials and Methods:	1794		
Results:	1896		
Discussion:	1674		
Conclusions	160		
Acknowledgements:	51		
Funding:	47		
Author Contribution:	53		

26

27 **Summary**

28

29 • Environmental stresses can result in a wide range of physiological and molecular responses
30 in plants. These responses can also impact epigenetic information in genomes especially
31 at the level of DNA methylation. DNA methylation is the hallmark heritable epigenetic
32 modification and plays a key role in silencing transposable elements (TEs). Although DNA
33 methylation is an essential epigenetic mechanism, fundamental aspects of its contribution
34 to stress responses and adaptation remain obscure.

35 • We investigated epigenome dynamics of wild strawberry (*Fragaria vesca*) in response to
36 variable environmental conditions at DNA methylation level. *F. vesca* methylome
37 responded with great plasticity to ecologically relevant abiotic and hormonal stresses.
38 Thermal stress resulted in substantial genome-wide loss of DNA methylation. Notably, all
39 tested stress conditions resulted in marked hot spots of differential DNA methylation near
40 centromeric or pericentromeric regions, particularly in non-symmetrical DNA methylation
41 context. Additionally, we identified differentially methylated regions (DMRs) within
42 promoter regions of transcription factor (TF) superfamilies involved in plant stress-
43 response and assessed the effects of these changes on gene expression.

44 • These findings improve our understanding on stress-response at the epigenome level by
45 highlighting the correlation between DNA methylation, TEs and gene expression
46 regulation in plants subjected to a broad range of environmental stresses.

47 **Keywords:**

48

49 epigenetics, stress response, transposable elements, transcription factors, centromeres

50

51 **Introduction**

52

53 Plants in natural environments are exposed to multiple stimuli, including numerous biotic and
54 abiotic stresses that make it necessary for plants to develop strategies to rapidly adapt. According
55 to the Global Climate Report 2020, the past 10 years were the warmest recorded around the globe
56 in our era. The greater temperature variability has resulted in both droughts and extreme
57 precipitations, affecting not only natural plant populations but also crop production (WMO, 2021).
58 In order to face these challenges, we need to better understand the mechanisms which allow plants
59 to rapidly adapt and evolve to better cope with increasing climate change-related stresses. Recent

60 advances in genome sequencing have revealed how dynamic plant genomes can be under stressful
61 scenarios (Kersey, 2019; Nguyen *et al.*, 2019, Roquis 2021). This dynamism can be attributed to
62 both genetic and epigenetic mechanisms which can contribute to specific traits (Varotto *et al.*,
63 2020; Wang *et al.*, 2019). However, how epigenetic information is influenced by stresses
64 (Quadrana & Colot, 2016; Lämke & Bäurle, 2017; MacKelprang & Lemaux, 2020; Varotto *et al.*,
65 2020) and whether these can contribute to adaptation requires a better understanding. DNA
66 methylation is an epigenetic mark which exists in three sequence contexts in plants: CG, CHG,
67 and CHH (H = A, C, or T). Each of them is regulated by distinct, but also interconnected silencing
68 mechanisms (Law & Jacobsen, 2010; Sahu *et al.*, 2013; Matzke & Mosher, 2014). Symmetric
69 methylation in the CG sequence context (mCG) has been found to be enriched in gene bodies but
70 the biological function of gene body methylation (gbM) remains unclear (Bewick & Schmitz,
71 2017; Bewick *et al.*, 2019). mCG is highly heritable and able to persist over many generations.
72 Conversely, DNA methylation in the CHG (mCHG) and CHH (mCHH) sequence contexts show
73 a lower stability (Becker *et al.*, 2011; Kuhlmann *et al.*, 2014; Schmitz *et al.*, 2011; Williams &
74 Gehring, 2017). DNA methylation is a hallmark epigenetic modification, contributing to the
75 regulation of many biological processes such as genome stability, definition of euchromatin and
76 heterochromatin, control of gene expression, and, most importantly, silencing of transposable
77 elements (TEs) (Bewick & Schmitz, 2017; Bucher *et al.*, 2012; Zhang *et al.*, 2018). Studies of
78 DNA methylation variability in natural *Arabidopsis* accessions have shown a clear correlation
79 between epigenomic changes in coding and non-coding genomic regions and environmental
80 stimuli, suggesting a role for DNA methylation in adaptation (Kawakatsu *et al.*, 2016). More
81 generally, it has been found that DNA methylation changes may be implicated in morphological
82 changes in response to different climates in plants (Guarino *et al.*, 2015; González *et al.*, 2018).
83 However, whether stress-induced methylome alterations at individual loci or across the entire
84 genome contribute to heritable changes in DNA methylation patterns and adaptation remains
85 uncertain.

86 A large fraction of the genome-wide observations on the functional properties of DNA methylation
87 in unfavorable growth conditions have been carried out on *Arabidopsis* (van Dijk *et al.*, 2010;
88 Colaneri & Jones, 2013; Jiang *et al.*, 2014; Shen *et al.*, 2014). However, its genome composition
89 differs significantly from cultivated crops that are characterized by larger genomes such as wheat,
90 maize or sugarcane (Niederhuth *et al.*, 2016; Vidalis *et al.*, 2016). Indeed, genomic DNA

91 methylation content is very low in Arabidopsis (Alonso *et al.*, 2015). Woodland strawberry
92 (*Fragaria vesca*, diploid, 219 Mb, $2n=2x=14$) (Edger *et al.*, 2018) is an interesting model for the
93 study of DNA methylation because it regulates key developmental traits of this species, including
94 seed dormancy (Zhang *et al.*, 2012) and fruit ripening (Cheng *et al.*, 2018). A notable example
95 concerning environmental impacts on DNA methylation is the documented loss of methylation at
96 TEs at high altitudes and how it can contribute to local adaptation to local conditions in natural
97 populations of wild strawberry (De Kort *et al.*, 2020; Sammarco *et al.*, 2022).

98
99 Here, we wanted to assess how stresses influence DNA methylation in *F. vesca* which has a
100 genome roughly twice as large as that of Arabidopsis, and at the same time offers advantages for
101 functional genomic and epigenomic studies compared to genetically complex cultivated octoploid
102 strawberry (*F. x ananassa*) ($2n=8x=56$) (Edger *et al.*, 2019; Shulaev *et al.*, 2011; Vitte *et al.*, 2014).
103 We present high-resolution data describing the impact of a diverse set of stresses on DNA
104 methylation in *F. vesca*. Depending on the stress conditions, we found that *F. vesca* can respond
105 with global and/or local changes in DNA methylation. Notably, these changes impact key
106 transcription factors (TFs) such as APETALA2/ethylene-responsive element binding factors
107 (*AP2/EREBP*) but also stress specific TFs such as heat shock transcription factors (*HSFs*).
108 Surprisingly, we find that all stresses have an impact on DNA methylation in centromeric or
109 pericentromeric regions implying that these genomic regions may act as stress-responsive
110 rheostats. Finally, we describe the DNA methylation dynamics at TE flanking regions as a strategy
111 to maintain homeostasis during stress responses.

112

113 **Materials and Methods**

114 **Plant growth and material**

115 All strawberry plants used in this study were a homozygous cultivated near-isogenic line (NIL),
116 Fb2:39–47, *F. vesca* cv. *Reine des Vallées* (RV), possessing the “r” locus on chromosome 2 which
117 causes this accession to propagate vegetatively through stolon development (Urrutia *et al.*, 2015).
118 Seeds from a single founder plant were germinated in water over Whatman filter paper for two
119 weeks and transferred to 50% MS medium (Murashige & Skoog, 1962) (Duscheffa cat# M0222),
120 30% sucrose, and 2% phytigel (Sigma-Aldrich cat# P8169) and grown for 4 weeks prior to stress.

121

122 **Stress assays**

123 One-month-old seedlings on agarose plates were exposed to different stresses under long-day
124 conditions (16 h light 24°C/8 h dark 21 °C) in plant growth chambers (Panasonic, phcbi: MLR-
125 352/MLR-352H). The seedling age was optimized to assure stress tolerance. For salt and drought
126 stress, one-month-old plantlets were transferred to MS media supplemented with 100 mM sodium
127 chloride (NaCl) (Sigma-Aldrich, cat# S9888) and 5% polyethylene glycol (PEG-6000) (-0.05
128 MPa) (Sigma-Aldrich, cat# P7181), respectively. For cold and heat stresses, plants were initially
129 grown as described above. The plates were then transferred to either 6°C or 37°C chambers. High
130 light was induced by 20,000 lx of illuminance ($460 \mu\text{mol s}^{-1} \text{m}^{-2}$) and low light with 80% sunblock
131 black net leading to 4,000 lx of illuminance ($92 \mu\text{mol s}^{-1} \text{m}^{-2}$). To simulate a hormone stress, MS
132 medium was supplemented with 0.5 mM salicylic acid (SA) (Sigma-Aldrich, cat# 247588). All
133 stress assays were carried out for 2 weeks with 2 recovery days after one week. For sampling, roots
134 were removed from 5 pooled plants for each treatment group (3 biological replicates) and harvested
135 in 1.5 mL tubes between 9:00 a.m. and 11:00 a.m. and immediately flash-frozen in liquid nitrogen
136 and stored at -80°C.

137

138 **Genome sequencing and assembly NIL Fb2**

139 Genomic DNA from strawberry plants was extracted by a Hexadecyltrimethylammonium bromide
140 (Cetrimonium bromide, CTAB) modified protocol (Healey *et al.*, 2014) and purified with
141 Agencourt AMPure XP beads (cat# A63880). Long-read sequencing was performed for genome
142 assembly; Genomic DNA by Ligation (Oxford Nanopore, cat# SQK-LSK109) library was
143 prepared as described by the manufacturer and sequenced on a MinION for 72 h (Oxford
144 Nanopore).

145

146 **Reference genome polishing**

147 Reads obtained from nanopore were filtered with Filtlong v0.2.1
148 (<https://github.com/rrwick/Filtlong>) using --min_mean_q 80 and --min_length 200. Cleaned reads
149 were then aligned to the most recent version of the *F. vesca* genome v4.0.a1 (Edger *et al.*, 2018),
150 with the annotation of *F. vesca* genome v4.0.a2 downloaded from the Genome Database for
151 Rosaceae (GDR) (<https://www.rosaceae.org/species/fragaria-vesca/genome-v4.0.a2>) (Jung *et al.*,
152 2019), using minimap2 v2.21 (Li, 2018) with parameters -aLx map-ont --MD -Y. The generated

153 BAM file was then sorted and indexed with samtools v1.11 (Li *et al.*, 2009). We used mosdepth
154 v0.3.1 (Pedersen & Quinlan, 2018) to verify that coverage on chromosomal scaffolds was over 50
155 X. Sniffles v1.0.12a (Sedlazeck *et al.*, 2018) with parameters `-s 10 -r 1000 -q 20 --genotype -l 30`
156 `-d 1000` was used to detect structural variations larger than 30 bp. We observed that larger
157 structural variants (SV) were most likely falsely identified due to misalignments in regions with
158 gaps or Ns, therefore the VCF files obtained from Sniffles were sorted and filtered with BCFtools
159 v1.14 (Danecek *et al.*, 2021) to keep only SV with less than 200 kb, supported by 10 or more reads
160 and with allelic frequencies above 0.8 to isolate homozygous changes. The complete filtering
161 command used was `"bcftools view -q 0.8 -Oz -i '(SVTYPE = "DUP" || SVTYPE = "INS" ||`
162 `SVTYPE = "DEL" || SVTYPE = "TRA" || SVTYPE = "INV" || SVTYPE = "INVDUP") &&`
163 `%FILTER = "PASS" && FMT/DV>9 && SVLEN>29 && SVLEN<200000' "`

164
165 From the VCF listing all the structural variants that we detected in our *F. vesca* accession, we
166 generated a substituted genome version based on the reference *F. vesca* genome v.4.0.a2. The
167 reference genome was first indexed with samtools faidx v1.11 (Danecek *et al.*, 2021) and a
168 sequence dictionary was generated with Picard CreateSequenceDictionary v2.25.6
169 (<https://broadinstitute.github.io/picard>). The VCF containing the SV produced from our Nanopore
170 sequencing was also indexed with gatk (Van der Auwera GA & O'Connor BD, 2020)
171 IndexFeatureFile v4.2.0.0 ([https://gatk.broadinstitute.org/hc/en-us/articles/360037262651-](https://gatk.broadinstitute.org/hc/en-us/articles/360037262651-IndexFeatureFile)
172 [IndexFeatureFile](https://gatk.broadinstitute.org/hc/en-us/articles/360037594571-FastaAlternateReferenceMaker)). FastaAlternateReferenceMaker v4.2.0.0 ([https://gatk.broadinstitute.org/hc/en-](https://gatk.broadinstitute.org/hc/en-us/articles/360037594571-FastaAlternateReferenceMaker)
173 [us/articles/360037594571-FastaAlternateReferenceMaker](https://gatk.broadinstitute.org/hc/en-us/articles/360037594571-FastaAlternateReferenceMaker)) was then run with the reference
174 genome and the VCF file to generate a substituted genome representative of our *Fragaria*
175 accession (Fb2).

176
177 As substituting our genome with the detected structural variants changes genomic coordinates, we
178 also corrected the public GFF genome annotation of *F. vesca* (Y, Pi, Gao, Liu, & Kang, 2019)
179 using liftoff v1.6.1 (Shumate & Salzberg, 2021). Liftoff also detects and annotates duplications
180 within the substituted genome.

181
182 Transposable elements annotation was carried out using the EDTA transposable element
183 annotation pipeline v. 1.9.6 (Ou *et al.*, 2019) on the substituted genome using default parameters.

184 The DOI for the *Fragaria vesca* Fb2:39–47 genome is: 10.5281/zenodo.6141713.

185

186 **Whole-genome bisulfite sequencing (WGBS)**

187 A modified CTAB DNA extraction protocol was performed using frozen above-ground tissues
188 (Healey *et al.*, 2014). DNA libraries were generated using the NEBNext Ultra II DNA Library
189 Prep Kit (New England Biolabs, cat# E7103S) according to the manufacturer's instructions with
190 the following modification for bisulfite treatment. DNA was sheared to 350 bp using a Covaris S2
191 instrument. The bisulfite treatment step using the EZ DNA Methylation-Gold kit (Zymo Research,
192 cat# D5007) was inserted after the adaptor ligation. After clean-up of the bisulfite conversion
193 reaction, library enrichment was done using Kapa Hifi Uracil+ DNA polymerase (Kapa
194 Biosystems, cat# KK1512) for 12 PCR cycles, using the 96 single-index NEBNext Multiplex
195 Oligos for Illumina (New England Biolabs, cat# E7335S). Paired-end reads were obtained on an
196 Illumina (150 bps) NovaSeq6000 instrument at Novogene (Hongkong, China).

197

198 **Processing and alignment of bisulfite-converted reads**

199 Sequencing data was analyzed by data collection software from read alignment to DNA
200 methylation analysis: EpiDiverse/wgbs pipeline (Nunn *et al.*, 2021). The pipeline included quality
201 control using FastQC v.0.11.9 (<http://www.bioinformatics.babraham.ac.uk/projects/fastqc/>) and
202 Cutadapt v.3.5 (<https://github.com/marcelm/cutadapt/>). Genome mapping was performed using
203 *erne-bs5* v.2.1.1 (Prezza *et al.*, 2012) with default parameters to generate the BAM files.
204 Methylation calling and methylation bias correction was performed with MethylDackel v.0.6.1
205 (<https://github.com/dpryan79/MethylDackel>) with only uniquely-mapping reads. The pipeline
206 used Nextflow v20.07.1 to run multitask in parallel. Because plant chloroplast DNA are not
207 methylated (Fojtová *et al.*, 2001), reads originating from those sequenced were used to evaluate
208 the bisulfite conversion rate. The pipeline is available at <https://github.com/EpiDiverse/wgbs>. An
209 average of 82,771,701 reads (~ 50X coverage) were produced per sample, of which 81% mapped
210 properly to the *F. vesca* genome. The average non-bisulfite conversion rate among the samples
211 was 0.10 (See Table S1 for more details). To calculate global methylation ratios, output files from
212 wgbs pipeline were pre-filtered for a minimum coverage of 5 reads using awk command and only
213 the common cytosine positions were kept among all the samples using bedtools 2.28.0. The data
214 were tested for statistical significance with an unpaired Student's t-test. $p < 0.05$ was selected as

215 the point of minimal statistical significance in all the analyses. R-packages ggplot2 v.3.3.5 and
216 gplots v.3.1.1 were used for the visualization of the results.

217

218 The Bisulfite-sequencing data from this study have been submitted to European Nucleotide
219 Archive (ENA, www.ebi.ac.uk/ena/, accessed on ERP135585) under the project PRJEB50996,
220 raw read fastq accessions under ERR8684931:ERR8684954.

221

222 **Identification of differentially methylated regions (DMRs)**

223 First, bedGraph files from wgbs pipeline were pre-filtered for a minimum coverage of 5 reads
224 using awk command. These output files were then used as input for the EpiDiverse/dmr
225 bioinformatics analysis pipeline for non-model plant species to define DMRs (Nunn *et al.*, 2021)
226 with default parameters (minimum coverage threshold 5; maximum q-value 0.05; minimum
227 differential methylation level 10%; 10 as minimum number of Cs; Minimum distance (bp) between
228 Cs that are not to be considered as part of the same DMR is 146 bp). The pipeline uses metilene
229 v.0.2.6.1 (<https://www.bioinf.uni-leipzig.de/Software/metilene/>) for pairwise comparison between
230 groups and R-packages ggplot2 v.3.3.5 and gplots v.3.1.1, for visualization results (Fig. S1). Based
231 on our *F. vesca* genome transcript annotation and methylation data (overlapped regions with DNA
232 methylation cytosines and DMRs), we detected the methylated genes, promoters, 3' UTRs, 5'UTR
233 and transposable elements in strawberry. Global DNA methylation and DMR plots were performed
234 with R-package ggplot2. Gene analyses by methylation patterns and analysis of per-family TE
235 DNA methylation profiles were performed with deepTools v.3.5.0 (Ramírez *et al.*, 2014). DMRs
236 comparison between treatments were done by the Venn diagram v.1.7.0 R-package.

237 We produced several genome browsers tracks with DMRs that we integrated in our local
238 instance of JBrowse available at the following url:

239 https://jbrowse.agroscope.info/jbrowse/?data=fragaria_sub. The bed files of the DMRs can be
240 downloaded here: 10.5281/zenodo.6141713

241

242 **Gene Ontology (GO) enrichment of differentially methylated genes**

243 All methylated genes were annotated based on GO annotation downloaded from the Genome
244 Database for Rosaceae (GDR)

245 (<https://www.rosaceae.org/species/fragaria-vesca/genome-v4.0.a2>).

246 To better understand the potential function of the differentially methylated genes, GO functional
247 classification of these genes was performed by AgriGO program v1.2 (Tian *et al.*, 2017). Genes
248 and promoters were classified by genes contained hypo and hypermethylated DMRs. The GO slim
249 library was used as reference GO reference type. Fisher's exact test p-values were calculated for
250 over-representation of the differential methylated genes in all GO categories and Hochberg (FDR)
251 as multi-test adjust method. GO terms with $p < 0.05$ were considered as significantly enriched.

252

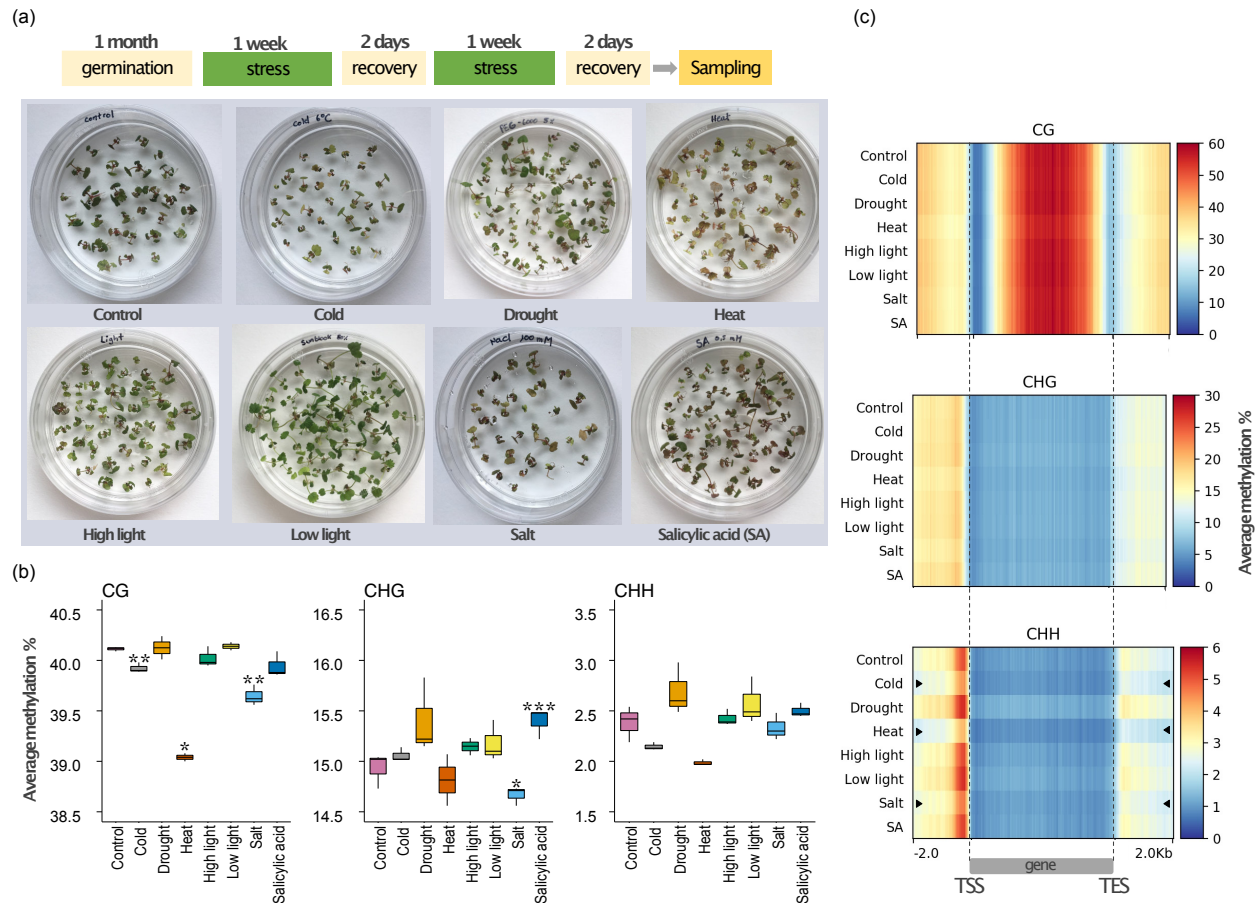
253 **Real-time Quantitative PCR Analysis**

254 One-month-old seedlings after heat and salt stress assays (as described above) were collected. For
255 sampling, roots were removed from 5 pooled plants for each treatment (3 biological replicates)
256 and harvested in 1.5 mL tubes between 9:00 a.m. and 11:00 a.m. and immediately flash-frozen in
257 liquid nitrogen and stored at -80°C . RNA was extracted using NucleoSpin RNA Plus, Mini kit for
258 RNA purification with DNA removal column (Macherey-Nagel, cat# 740984.50). cDNA synthesis
259 was performed using EvoScript Universal cDNA Master (Roche, cat#07912374001). The
260 strawberry Elongation factor 1 (*EF1*) (Amil-Ruiz *et al.*, 2013) gene was used as a control to
261 normalize the amount of cDNA used from each sample. Eurofins PCR Primer Design Tool
262 (<https://eurofinsgenomics.eu/en/ecom/tools/pcr-primer-design/>) was used to design gene-specific
263 primers for *AP2/EREBP* and *FvHSF* genes (Table S2). Real-time quantitative PCR was carried
264 out using LightCycler 480 SYBR. Green I Master mix (Roche, Cat#04707516001) on a
265 LightCycler® 480 Instrument (F. Hoffmann-La Roche Ltd) with a final volume of $20\mu\text{l}$ per
266 reaction. Each reaction mixture contained $7\mu\text{l}$ of Water (PCR grade), $1.0\mu\text{l}$ cDNA template, $1.0\mu\text{l}$
267 of each primer ($0.5\mu\text{M}$), and $10\mu\text{l}$ Master Mix ($2\times$). Each reaction was performed in triplicate.
268 Relative gene expression was determined using *EF1* gene as housekeeping gene and analyzed
269 using the qGene protocol of Normalized Expression method (Muller *et al.*, 2002). The primers
270 used for real-time RT-qPCR are listed in Table S2. The data are presented as the mean \pm standard
271 error and were tested for statistical significance with an unpaired Student's t-test. The $p < 0.05$ was
272 selected as the point of minimal statistical significance in all the analyses.

273 **Results**

274 **Stress-induced DNA methylation dynamics in *F. vesca***

275 To evaluate how DNA methylation is altered under diverse plant growth environments, *F. vesca*
276 seedlings were cultivated in a growth chamber *in vitro* for 1 month and then transferred to one of
277 seven different stress environments (Fig. 1a). The treatments represented stress conditions which
278 affect normal plant development (Lämke & Bäurle, 2017): cold, heat, drought, high and low light,
279 and salt as abiotic stresses; salicylic acid (SA) as hormone stress. Control plants were grown on
280 MS medium without stress treatment. After one week of stress exposure, the plants were moved
281 to control conditions for two days to ensure survival. Then, plants were stressed for a second week
282 and finally, moved back to control conditions for two days of recovery (Fig. 1a, see **Materials and**
283 **Methods** for details). To assess genome-wide DNA methylation levels, DNA was extracted from
284 these plants and submitted to whole genome bisulfite sequencing (WGBS, 20x genome coverage)
285 (Table S1). We carried out a global quantification of DNA methylation in the three sequence
286 contexts (CG, CHG and CHH). First, we combined all bedGraph files of the individual samples
287 into a unionbedg file and filtered the cytosine positions without sequencing coverage and
288 calculated the average DNA methylation levels. Overall, the global DNA methylation levels in all
289 stress conditions were similar (Fig. 1b). *F. vesca* seedlings in control conditions had 40.11% mCG,
290 14.93% mCHG and 2.38% mCHH. We found substantial decreases of 0.5%, 3.2% and 1.1% for
291 global mCG after cold, heat and salt stress, respectively (Fig. 1b). In addition, we observed a
292 significant global mCHG decrease of 1.8% in salt and an increase of 3.1% in the presence of SA.
293 We did not detect significant changes in global mCHH level. To assess methylation variation in
294 genic and non-genic sequences, we screened the methylome data in all three contexts separately
295 in three regions: 2 kb upstream of genes, along the gene body, and 2 kb downstream of genes
296 within a 100-bp sliding window (Fig. 1c). In contrast to the global analysis, here we observed a
297 higher local DNA methylation variability in the CHH context at the transcription start and end
298 sites (TSS and TES, correspondingly) compared to the other two contexts. Notably for CHH
299 context, cold and heat stress resulted in hypomethylation at the TSS, TES and over the gene body
300 (Fig. 1c). We extracted genes with body methylation (gbM) similarly to the parameters defined
301 previously (Bewick *et al.*, 2019) filtering for at least 20 CGs and a methylation level above the
302 median value. Genes containing gbM showed low variability in all the conditions (Fig. S2).



303
 304 **Fig. 1 Effect of abiotic and hormone stresses on genome-wide DNA methylation levels in *F.***
 305 ***vesca*.** (a) Top: Scheme of stress treatment time course. Bottom: Photographs of plates with one-
 306 month-old plants grown under different stress conditions (cold, drought, heat, high and low
 307 intensity of light, salt, and salicylic acid). (b) Average DNA methylation levels for each cytosine
 308 context (CG, CHG, CHH) between normal and stress conditions (only common cytosines positions
 309 among all samples were considered that had a minimum coverage of 5 reads). Asterisks indicate
 310 levels of significance between treated and control plants: *, p-value < 0.05; **, p-value < 0.01;
 311 ***, p-value < 0.001 (unpaired two-tailed Student's t-test). (c) Heat maps showing distribution of
 312 DNA methylation (top: CG, middle: CHG, and bottom: CHH context) around genes with and
 313 without stress (Control). Mean of the average methylation percentage (within a sliding 100-bp
 314 window) was plotted 2 kb upstream of TSS, over the gene body and 2 kb downstream of TES.
 315 Black arrows highlight the samples in which a reduction of DNA methylation can be observed in
 316 the vicinity of TSS and TES sites.

317

318 **Stress particularly affects DNA methylation variability in the non-CG contexts in *F. vesca***

319 To explore the dynamics of DNA methylation at specific loci in detail, we assessed differentially
 320 methylated regions (DMRs) for each sequence context. DMRs were defined using metilene
 321 v.0.2.6.1 which uses an algorithm to identify a base-pair window through sequence segmentation
 322 with significant methylation differences (Jühling *et al.*, 2016) (See Materials and Methods for

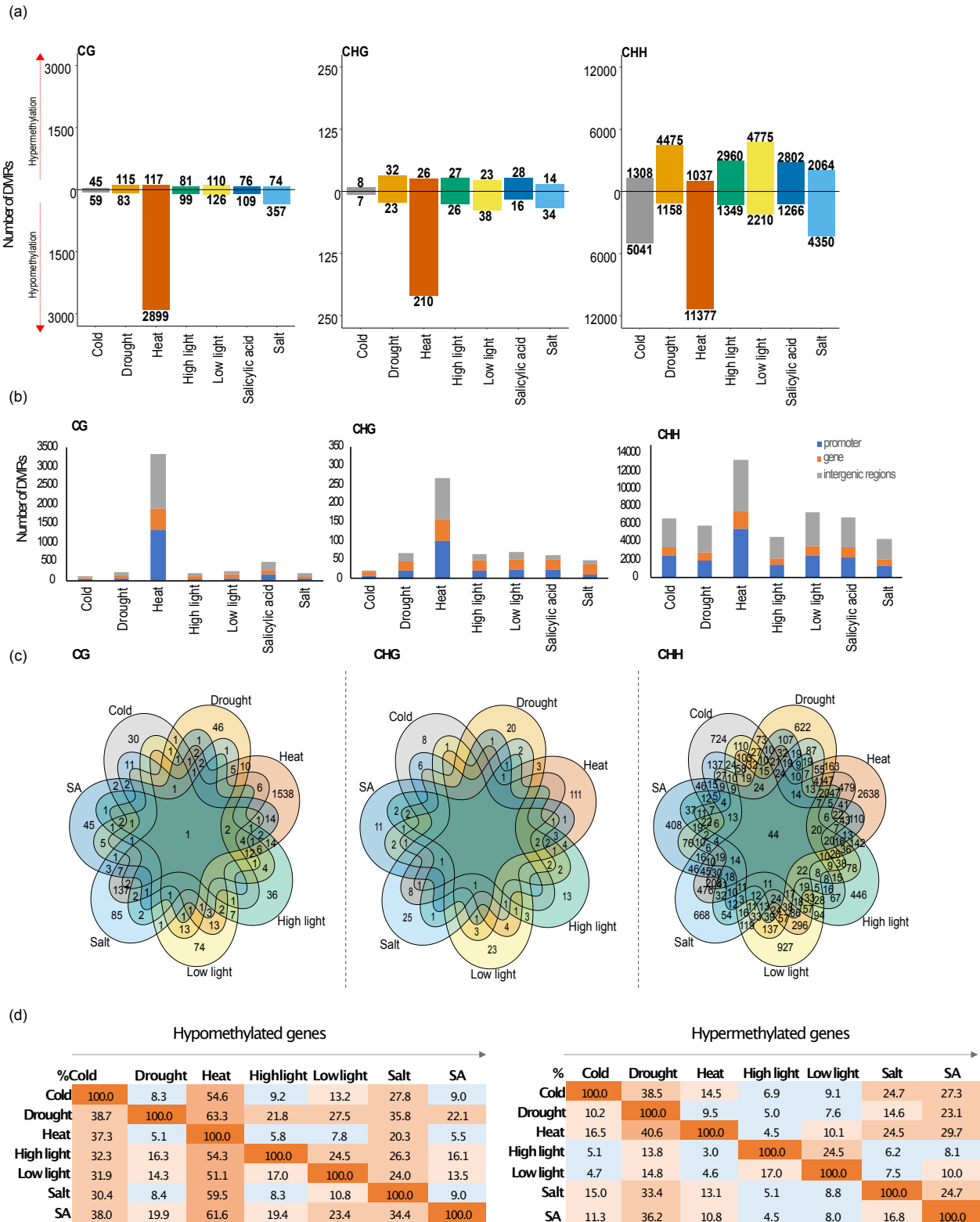
323 parameters). We compared the methylomes of plants submitted to each stress condition with the
324 methylomes from control plants. The majority of DMRs identified were in the CHH context for
325 all conditions, with a maximum of 12,414 DMRs under heat stress. Fewer DMRs were detected in
326 both CG sequence context, ranging from 104 (cold stress) to 3,016 (heat stress), and in the CHG
327 context, ranging from 15 (cold stress) to 236 (heat stress) (Fig. 2a, Table S3). In line with our
328 global DNA methylation analysis, most of the heat, cold and salt stress DMRs were
329 hypomethylated (hypoDMRs) relative to the control condition in all sequence contexts. For
330 drought, high light, low light, and SA stress, most of the DMRs showed hypermethylation
331 (hyperDMRs) in the CHH context (Fig. 2a). Next, to test whether genic and non-genic regions
332 were rich in DMRs, we qualified DMRs on their intersection with promoters (empirically defined
333 as 2 kb to 50 bp upstream TSS), gene bodies, and intergenic regions. The minimum overlap
334 required was 1bp. Many of the CG and CHG DMRs (30-44%, 45-60% respectively) were in genes,
335 while most of CHH DMRs (between 32-44%) were in promoters and intergenic regions (Fig. 2b).
336 In summary, abiotic and hormone stresses led to DNA methylation changes primarily in the CHH
337 context within promoters and intergenic regions. Overall, heat stress caused the most numerous
338 DNA methylation changes.

339

340 **Identification of stress-induced DNA methylation changes in genic regions**

341 To better understand the potential functional roles of the DMRs and the commonalities between
342 the different stresses, we focused our analysis on DMRs located within promoters and gene bodies
343 (Fig. 2c). We only identified one locus with a CG DMR (within *FvH4_6g40845* an unknown
344 protein) and 44 loci with CHH DMRs that were in common to all stress conditions (Fig. 2c, Fig.
345 S3). Comparing each stress data set of promoter and gene locations with hypo- and hyperDMRs
346 we noted that heat stress shared more loci with hypoDMRs with the other conditions than all other
347 comparisons (Fig. 2d, left). For example, 37.3% of loci with heat-stress hypoDMRs overlapped
348 with 54.6% of all hypoDMRs found under cold-stress. Conversely, drought stress resulted in the
349 highest number of genic loci with hyperDMRs shared with the other conditions. To illustrate,
350 40.6% of heat-stress hyperDMRs overlapped with 9.5% drought-stress hyperDMRs (Fig. 2d,
351 right). In order to identify potential functional roles for these DMRs, we performed a singular
352 enrichment analysis (SEA) using the AgriGO tool (Tian *et al.*, 2017) (see **Materials and**
353 **Methods**). *F. vesca* has around 34,000 genes but only 54% of which have been assigned a GO

354 number (Li *et al.*, 2019). For this reason, “unknown” annotated genes were omitted for this analysis
355 (Table S4). The analysis was based on the identified genic regions (gene and promoter) with DMRs
356 for each stress condition according to their methylation change (hypo- or hypermethylated). Plants
357 submitted to heat stress showed the largest variation in DNA methylation over genic regions. These
358 were enriched with hyperDMR-associated genes involved in the generation of precursors of
359 metabolites and energy. Genes with heat-stress induced hypoDMRs were enriched for
360 transcription factor (TF) activity, transcriptional regulators, and genes related to cellular
361 components (Table 1). We also found that cold stressed plants had hyperDMR-associated genes
362 enriched for transporter activity (Table 1).



363
 364 **Fig. 2 Differentially methylated regions in *F. vesca* seedlings grown at control and stress**
 365 **conditions.** (a) Number of stress-induced hyper- (hyperDMRs) and hypomethylated DMRs
 366 (hypoDMRs) separated by sequence context. (b) Distribution of DMRs in genomic features:
 367 promoter (2 kb to 50 bp upstream TSS), gene body, and intergenic regions. Minimum overlap

368 required: 1bp. (c) Venn diagrams of common promoter and genic regions containing hypo- and
 369 hyperDMRs per context among all the stress conditions. (d) Percentages of genic loci with hypo-
 370 and hyperDMRs which are shared among the stress conditions. Reading from left to the right
 371 (arrow). e. g. (Left block) 8.3% genic locations with cold-stressed hypoDMRs overlap with 38.7%
 372 genic locations with drought-stress induced hypoDMRs. (Right block) 24% genic loci with
 373 hyperDMRs from salt-stressed seedlings overlap with 11% genic loci with hyperDMRs resulting
 374 from SA treatment. Ascending intensity of block colors correlate with overlap percentages.

375 **Table 1. Gene ontology (GO) enrichment analysis of genic regions (gene and promoter) with**
 376 **DMRs.** GO enrichment of genes with hypo- and hyperDMRs caused by thermal stress. The genes
 377 are arranged according to their DMRs patterns.

Stress	Methylation	Description	FDR	Number in input list	Number in BG/Ref	Ontology
Cold	Hypermethylation	transporter activity	0.024	23	838	F
Heat	Hypermethylation	generation of precursor metabolites and energy	0.021	8	153	P
	Hypomethylation	transcription regulator activity	0.024	108	420	F
		transcription factor activity	0.02	99	380	F
		intracellular	0.03	504	2276	C
		cell part	0.03	849	3930	C
		cell	0.03	849	3930	C
		cytoplasm	0.03	239	1029	C

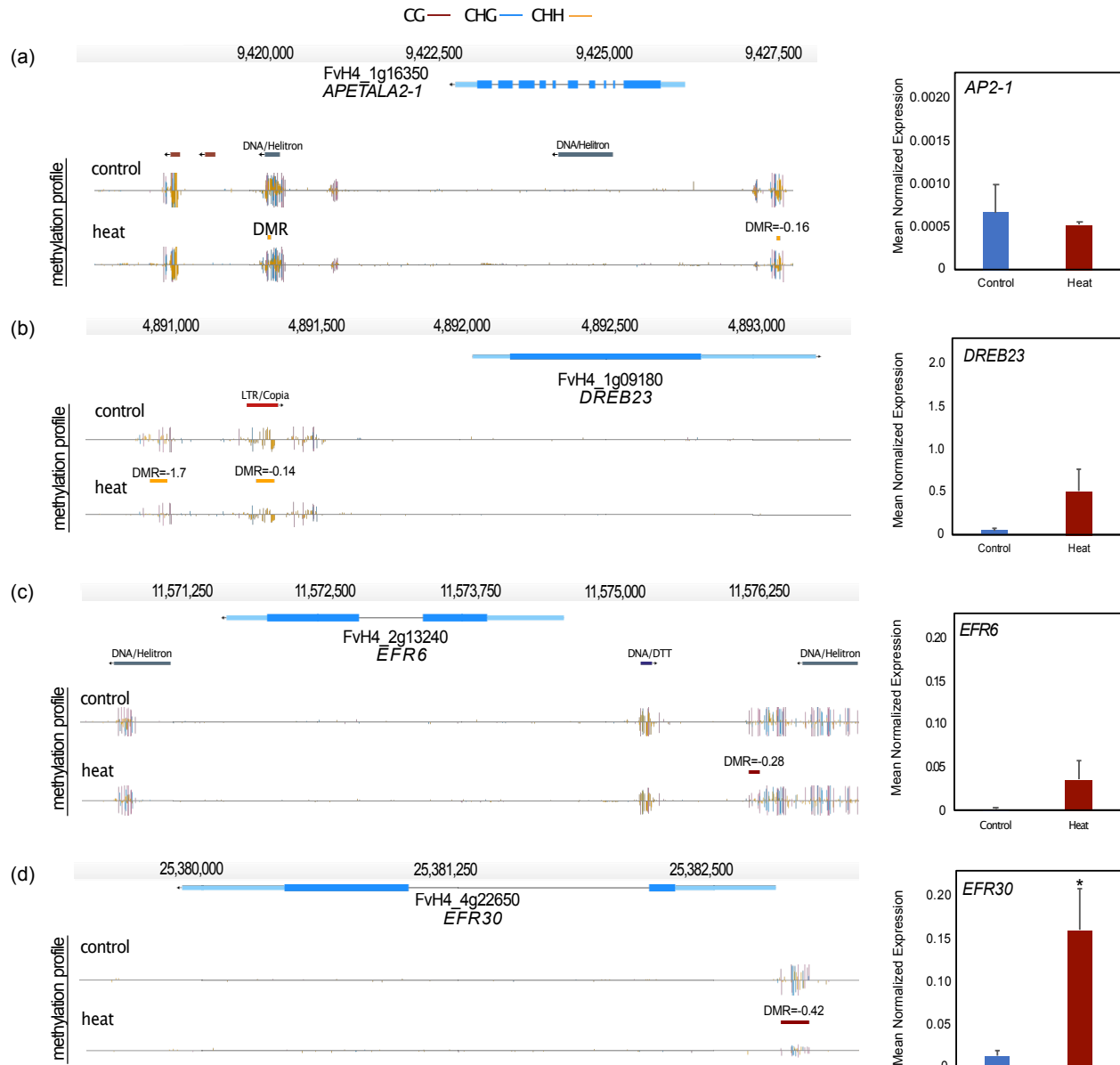
378 GO categories are listed with the false discovery rate-adjusted P-value <0.05. BG: background,
 379 Ref: reference, C: Cellular Component; F: Molecular Function; P: Biological process. Only well
 380 identified and annotated genes were included in the analysis.

381

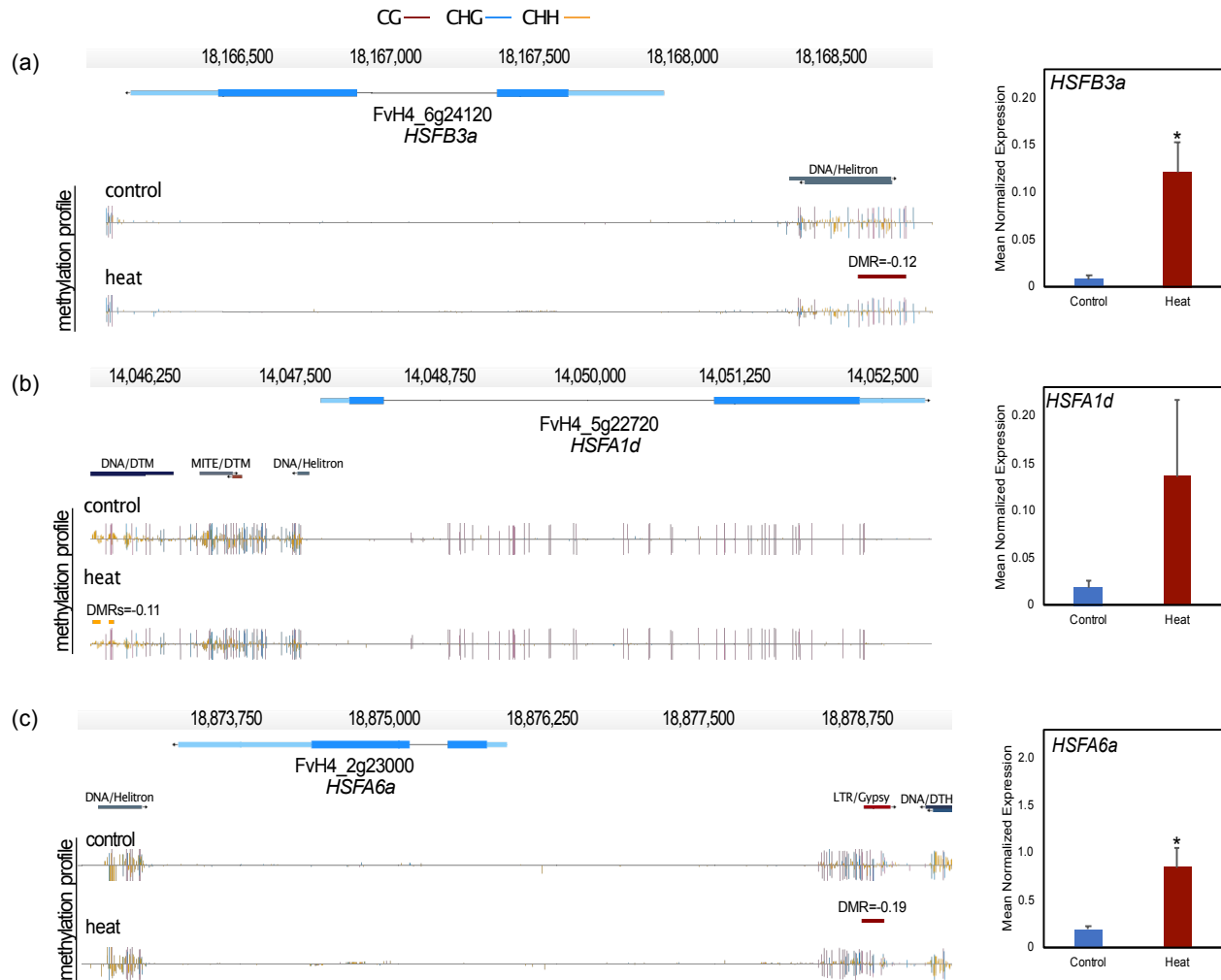
382 Heat stress induced hypomethylation at transcription factor coding genes

383 Transcription factors (TFs) play key roles in plant growth, development, and stress responses.
 384 Interestingly, we observed that heat stress resulted in an enrichment of hypoDMRs at promoters
 385 and genes related to TFs. Among 99 genes related to transcription factor activity (Table1), 31%
 386 were *AP2/EREBP* members and 4% heat shock transcription factors (*HSFs*). *AP2/EREBP*
 387 members (119 genes in total) have been characterized in the latest version of the *F. vesca* genome
 388 and are known to be involved in stress tolerance (Dong *et al.*, 2021; Xie *et al.*, 2019). To evaluate

389 the detailed DNA methylation changes at *AP2/EREBP* genes under different stress conditions, we
390 looked at the distribution of DNA methylation at those loci (Fig. S4a). We observed a noted
391 reduction in DNA methylation at the TSS in the CHH context for heat- and cold-stressed plants.
392 Combining all stress conditions, a total of 74 DMRs were identified within the promoter regions
393 of 44 *AP2/EREBP* genes (Table S5). The marked presence of DMRs within *AP2/EREBP*
394 promoters suggested a relationship between methylation and transcription. We therefore randomly
395 selected four members among each subgroup of the *AP2/EREBP* gene superfamily to detect
396 transcript levels by qRT-PCR analysis (Fig. 3). Even though heat-treated plants seemingly showed
397 higher transcript levels compared to the control plants, only *ERF30* gene was significantly up-
398 regulated (Fig. 3a). In addition, *ERF30* showed the highest methylation difference ratio (CG
399 DMR=-0.42) in its promoter. We also obtained similar results by analyzing the relationship
400 between methylation and expression of heat shock factors (*HSFs*). Initially, 14 *HSFs* have been
401 identified in *F. vesca* genome (Hu *et al.*, 2015); however, in the last genome annotation version
402 (Li *et al.*, 2019), we were able to identify 19 *HSFs* (Table S6). The distribution of methylation
403 over *HSFs* showed high variability in TSS and TES in CHH context compared gene bodies (Fig.
404 S4b). We identified 13 *HSFs* with DMRs within promoter regions mostly attributed to heat stress
405 (Table S6). For the functional expression analysis three genes were randomly selected (Fig. 4).
406 Hypomethylation in promoter regions of *HSFB3a* and *HSFA6a* showed a clear relationship with
407 significantly increased transcript levels after heat stress (Fig. 4a, c). Collectively, our data show
408 that heat stress induces loss of DNA methylation mostly at promoter regions of genes related to
409 specific TF families possibly influencing their transcription.



410
 411 **Fig. 3 Functional analysis of heat-stress DMRs within AP2/EREBP**
 412 **element binding protein (AP2/EREBP) superfamily genes.** Genome browser views of DMRs
 413 located in promoter regions of AP2/EREBP genes and bar plots indicate expression ratios using
 414 three biological replicates of pooled seedlings. (a) AP2-1 (APETALA2-1), (b) FvDREB23
 415 (dehydration-responsive element binding 23), (c) ERF6 (ethylene-responsive binding factor 6), (d)
 416 ERF30 (ethylene-responsive binding factor 30). Depicted are genes structures (top panels, UTRs
 417 in light blue, exons in blue), TEs (red and dark blue) and DNA methylation levels (histograms).
 418 Boxes above the histograms indicate identified DMRs with methylation difference ratios (color
 419 codes for DNA methylation: red for CG, blue for CHG and yellow for CHH contexts). Error bars
 420 in the plots indicate Standard error. Asterisks indicate levels of significance between treated and
 421 non-treated plants: *, p-value < 0.05 (unpaired two-tailed Student's t-test).



422
 423 **Fig. 4 Correlation between heat-stress hypoDMRs and up-regulation of heat shock**
 424 **transcription factors (*HSF*) expression.** Genome browser views of DMRs present in located in
 425 promoter regions of HSF. (a) *HSFB3a* (heat shock transcription factor B 3a), (b) *HSFA1d* (heat
 426 shock transcription factor A 1d), (c) *HSFA6a* (heat shock transcription factor A 6a). Depicted are
 427 gene structures (top panels, UTRs in light blue, exons in blue), TEs (red and dark blue) and DNA
 428 methylation levels (histograms). Boxes above the histograms indicate identified DMRs with
 429 methylation difference ratios (color codes for DNA methylation: red for CG, blue for CHG and
 430 yellow for CHH contexts). Error bars in the plots indicate Standard error. Asterisks indicate levels
 431 of significance between treated and non-treated plants: *, p-value < 0.05 (unpaired two-tailed
 432 Student's t-test).

433

434 Stress leads to distinct methylation changes at transposable elements (TEs)

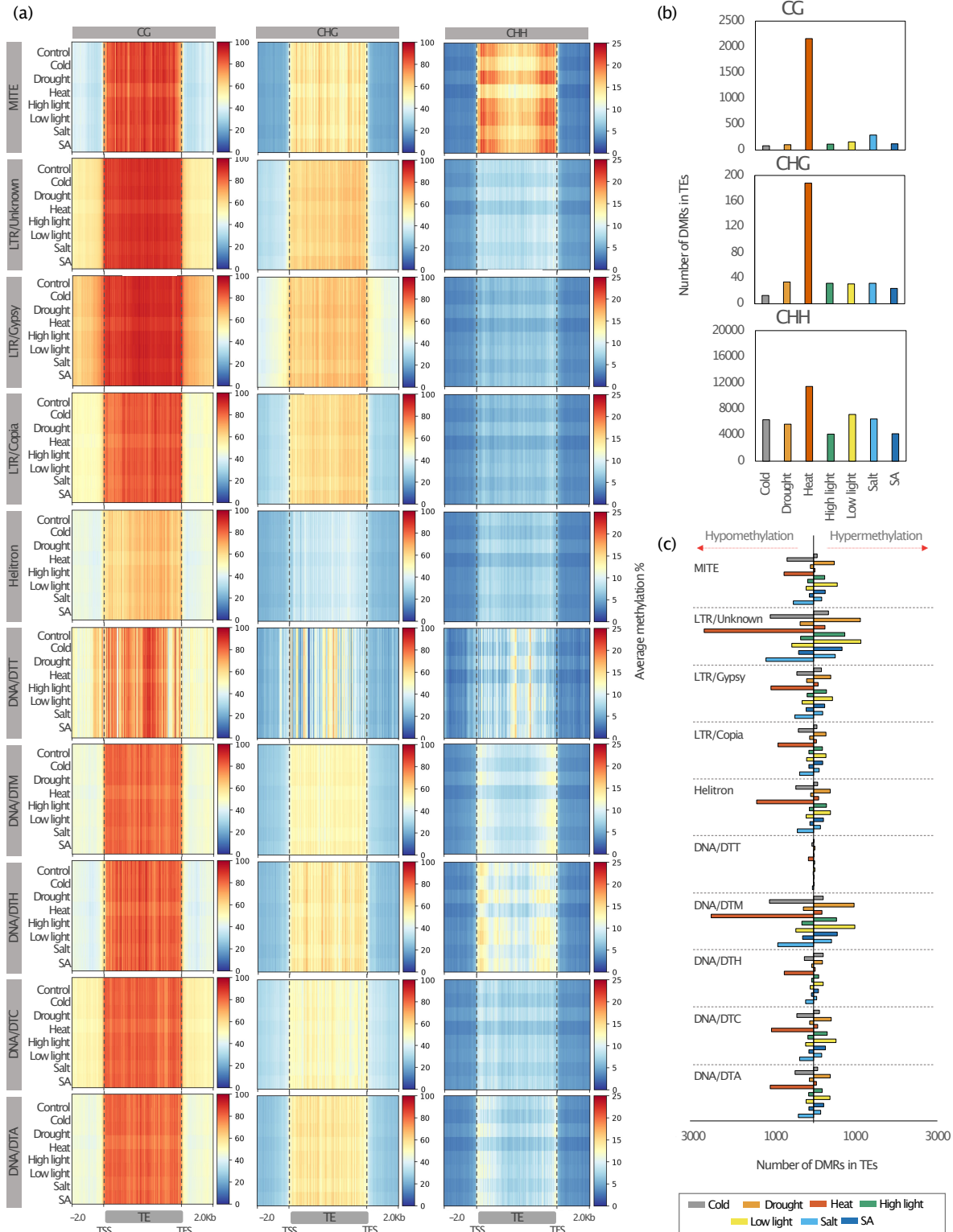
435 Since one of the most important functions of DNA methylation is to repress TE transcription and
 436 mobility (Bucher *et al.*, 2012; Deniz *et al.*, 2019; Fedoroff, 2012; Zhang *et al.*, 2018), we
 437 investigated the effect of stress on DNA methylation at TEs. To describe the variation in DNA

438 methylation in TE bodies and their flanking regions we plotted DNA methylation profiles in all
439 three contexts. We used 50-bp sliding window: 2kb upstream, over the body and 2 kb downstream
440 (Fig. 5a). In general, all TE families showed high methylation levels in CG context; however,
441 DNA transposons such as the *Mariner* (DTT) and *Helitrons* superfamilies were characterized by
442 low DNA methylation levels in the CHG context. Notably, *Miniature Inverted-Repeat*
443 *Transposons* (MITEs) showed the highest DNA methylation levels in CHH context. For MITEs,
444 mCHH was distinctly reduced under cold, heat and salt stress (Fig. 5a). To assess significant
445 changes in DNA methylation at specific loci over TEs, we counted the number of DMRs within
446 TE annotations for each stress condition (Fig. 5b). The minimum overlap DMRs/TEs was 1bp. As
447 for genes, we identified the greatest number of DMRs within TEs in heat-stressed plants in all
448 cytosine contexts (Fig. 5b). Cold, heat, and salt stress displayed more hypoDMRs in TEs compared
449 to drought, low light, high light, and SA, which produced more hyperDMRs in TEs (Fig. 5c).
450 Although there was no specific TE family significantly enriched in DMRs, heat-stress resulted in
451 at least 12% of all MITES acquiring hypoDMRs (Fig. 5c, Table S7) and most of them were close
452 to genic regions (< 2kb upstream genes) (see Fig. 6 for examples). Overall, these results suggested
453 that DNA methylation dynamics among all TE members changed proportionally in all
454 superfamilies; nonetheless, the change regarding gain or loss of DNA methylation was clearly
455 defined by the applied stresses.

456

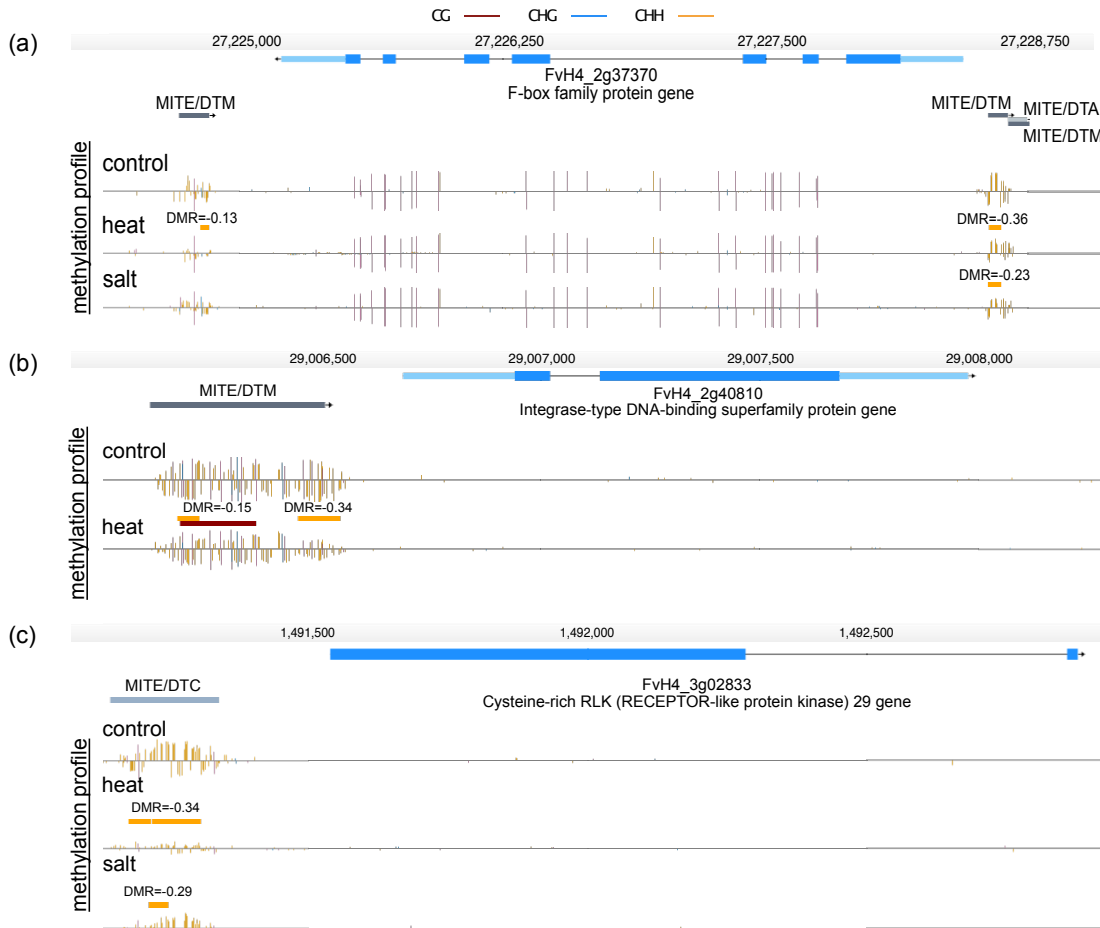
457 **DMRs are enriched in distinct regions of the *F. vesca* in the genome**

458 Even though genome-wide DNA methylation variation levels were low (Fig. 1b), we observed
459 regions in the genome that were enriched in DMRs in all stress conditions (Fig. 7a). Indeed, we
460 observed DMR hotspots in the *F. vesca* genome. Notably, the distribution showed a similar pattern
461 on all chromosomes independently of the stress conditions. The DMR density was not clearly
462 related to gene and TE density (Fig. 7b); nevertheless, when we analyzed individual TE families,
463 *Helitron* density hotspots showed a clear correlation with DMR density (Fig. 7). Currently, little
464 is known about the exact localization of centromeric and pericentromeric regions in strawberry (Li
465 *et al.*, 2018). However, it has been reported previously that centromeric regions can be enriched in
466 *Helitrons* in certain plant genomes (Xiong *et al.*, 2016). It is important to note here, that the
467 *Helitrons* themselves were not enriched in DMRs.

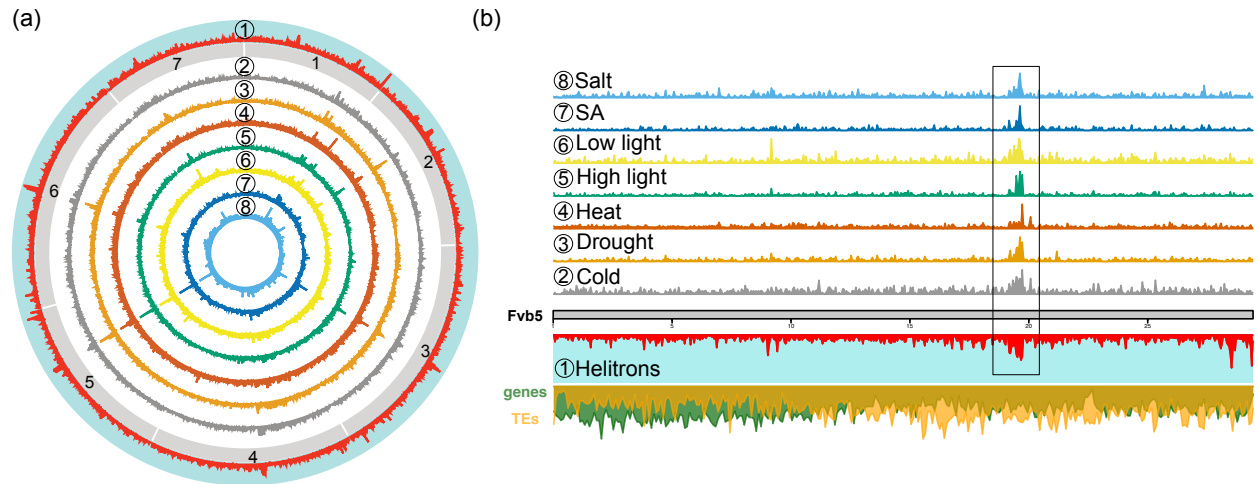


468
469 **Fig. 5 Association of stress-induced differentially methylated regions with transposable**
470 **elements in *F. vesca*.** (a) Heatmaps showing DNA methylation profiles for the all the TE families
471 separated by sequence context mCG (left), mCHG (center) and mCHH (right). The mean of the
472 average DNA methylation percentage (within a 50 bp sliding window) was plotted for the TE
473 bodies and 2 kb around the TSS and TES regions. (b) Number of stress induced DMRs in TEs per

474 sequence context. (c) Number of hypoDMRs (left) and hyperDMRs (right) within different TE
475 families. Class I elements (retrotransposons): *LTR-Copia*, *LTR-Gypsy*. Class II elements (DNA
476 transposons): TIR: *Tc1-Mariner* (DTT), *hAT* (DTA), *Mutator* (DTM), *PIF-Harbinger* (DTH),
477 *CACTA* (DTC); *Helitron*; *Miniature Inverted-Repeat Transposons* (MITEs). Upper char box
478 indicates the colors which represent each treatment.



479
480 **Fig. 6 Miniature Inverted-Repeat Transposons (MITEs) present hypomethylated regions**
481 **(DMRs) under abiotic stress conditions.** Genome browser views of DMRs present in MITEs
482 located near genes. (a) F-box family protein gene (FvH4_2g37370). (b) Integrase-type DNA
483 binding superfamily protein gene (FvH4_2g40810). (c) Cysteine-rich RLK (RECEPTOR-like
484 protein kinase) 29 (FvH4_3g02833). Depicted are genes structures (top panels, UTRs in light blue,
485 exons in blue), TEs (red and dark blue) and DNA methylation levels (histograms). Boxes above
486 the histograms indicate identified DMRs with methylation difference ratio (color codes for DNA
487 methylation: red for CG, blue for CHG and yellow for CHH contexts).



488
489

490 **Fig. 7 Genome-Wide distribution of DMR densities.** (a) Circa plot showing DMR densities on
491 all 7 strawberry chromosomes (gray boxes) for each stress condition (2. Cold, 3. Drought, 4. Heat,
492 5. High light, 6. Low light, 7. SA, and 8. Salt). *Helitron* density (1) in the genome is depicted on
493 the outer most circle in red with turquoise background. (b) DMR density depicted on chromosome
494 5 (Fvb5) displaying a common enrichment among all the stress conditions (left of the 20 Mb tick
495 mark). Below, the chromosome is indicated in grey, green shows gene density, yellow the TE
496 density and red Helitrons along the chromosome.

497

498 Discussion

499

500 Genome-wide DNA methylation patterns are altered under stressful environmental 501 conditions

502 Environmentally induced epigenetic changes include mechanisms that respond to abiotic or biotic
503 stress conditions in plants (Verhoeven *et al.*, 2016). DNA methylation variation might trigger
504 modifications in plant development and physiology contributing to phenotypic variability, thereby
505 presumably contributing to plant acclimation (Dubin *et al.*, 2015; Lämke & Bäurle, 2017; Xu *et*
506 *al.*, 2020; Zhang *et al.*, 2021). Here, we studied DNA methylation dynamics in *F. vesca* submitted
507 to two successive stress applications. Looking at the total DNA methylation levels in the three
508 different sequence contexts, we observed only slight variations among the different stress
509 conditions. However, by performing a DMR analysis we detected extensive differences at specific
510 loci especially in the CHH context. This is in agreement with studies which reported that mCHH
511 was most dynamic in response to different climates (Downen *et al.*, 2012; Dubin *et al.*, 2015;
512 Kenchanmane *et al.*, 2019). More specifically, in the case of *F. vesca*, altitude variations of natural
513 strawberry populations was found to be correlated with a high variability in DNA methylation in

514 the CHH context (De Kort *et al.*, 2020; Kort *et al.*, 2021). In our study, cold, heat, and salt stress
515 resulted in substantial local loss of DNA methylation in all sequence contexts, particularly in
516 regions close to TSS and TES sites in the *F. vesca* genome (Fig. 1c). Such DNA methylation
517 changes have been associated with different degrees of cold tolerance. Indeed, different crop
518 species such as maize, rice, cotton, and chickpea presented an increased number of
519 hypomethylated regions near abiotic stress response genes and transcription factors upon cold
520 stress (Fan *et al.*, 2013; Pan *et al.*, 2011; Rakei *et al.*, 2016; Shan *et al.*, 2013). Higher temperature
521 resulted in hypomethylation in different plant tissues, such as rice seeds, soybean roots, and
522 tobacco leaves, affecting plant growth by altering gene expression patterns in genes that control
523 biosynthesis and catabolism of phytohormones (Centomani *et al.*, 2015; Hossain *et al.*, 2017; Qian
524 *et al.*, 2019; Suriyasak *et al.*, 2021). In addition, salt stress induced epigenetic variation in
525 *Arabidopsis* have been shown to be partially transmitted to offspring, primarily via the female
526 germ line (Wibowo *et al.*, 2016). On the other hand, we noticed little gain of global DNA
527 methylation caused by different intensities of light or drought and SA stresses; yet causing a
528 considerable number of hyperDMRs in the CHH context. Different results were found in tomato
529 plants exposed to variable intensities of light which resulted in DNA hypomethylation and
530 transcriptional changes causing male-sterility (Omidvar & Fellner, 2015). However, drought stress
531 induced mCG and mCHG hypermethylation and a slight decrease in mCHH methylation in
532 mulberry (Li *et al.*, 2020). There is also evidence that drought, nitrogen-deficiency and heavy
533 metal stresses can result in heritable changes in DNA methylation levels across generations in rice
534 (Kou *et al.*, 2011; Ou *et al.*, 2012; Zheng *et al.*, 2013). Another study showed that DNA
535 methylation changes induced by hormone stresses via Jasmonic and Salicylic acid can be faithfully
536 transmitted to offspring by asexual reproduction in dandelions (Verhoeven *et al.*, 2010). Together,
537 these findings open the question of whether stress-induced DNA methylation changes found in *F.*
538 *vesca* can be maintain over generations through asexual (stolons) and sexual (seeds) reproduction.
539 An aspect we are currently intensively investigating.

540

541 **Different TE superfamilies show contrasted responses to stresses**

542 DNA methylation plays a key role in limiting transcriptional activation and mobilization of TEs
543 in order to ensure genome integrity (Slotkin & Martienssen, 2007; Bucher *et al.*, 2012; Deniz *et al.*
544 *et al.*, 2019). Indeed, TEs can be an important source of genetic and epigenetic variation that can

545 influence stress-responses (Naito *et al.*, 2009). Here, we wanted to better understand how different
546 TE superfamilies respond to the stresses we applied. Using this approach, we observed distinct
547 DNA methylation profiles at TEs depending on their superfamily and the applied stress conditions.
548 Overall, we found that *F. vesca* TEs are highly methylated in both, CG and CHG sequence
549 contexts. Similar results were observed in maize where LTR and TIR elements are highly
550 methylated under normal conditions (Noshay *et al.*, 2019). On the other hand, we noticed that
551 overall DNA methylation levels in the CHH context were lower and more variable among different
552 TE superfamilies and stress conditions, implying contrasted responses of TEs to stresses and that
553 these TEs are silenced by different transcriptional gene silencing pathways. These DNA
554 methylation changes could have direct physiological impacts as non-CG methylation seems to
555 create a boundary between genes and TEs (Kenchanmane *et al.*, 2019). For example, it has been
556 found that TEs located close to stress-induced genes in Arabidopsis and rice are silenced by
557 hypermethylation after phosphate starvation in order to prevent collateral activation of TE
558 transcription during stress (Secco *et al.*, 2015). In our study we found that heat stress affected
559 mCHH in the TE body of all TE superfamilies. MITES had the highest percentage of members
560 targeted by DMRs (Table S7). In addition, we noticed MITES to often be present in promoter
561 regions of genes with DMRs. A genome-wide transcriptional analysis would be needed to
562 generally conclude on whether the variation of DNA methylation in promoters might be stimulated
563 by the presence of MITES thereby contributing to gene expression control *in cis*. In line with these
564 observations, previous studies have highlighted the importance of MITES in genome evolution
565 and how MITE insertions in promoter regions can regulate the expression of genes in a wide
566 variety plant species such as maize, rice, and mulberry (Lu *et al.*, 2012; Wei *et al.*, 2014; Mao *et*
567 *al.*, 2015; Xin *et al.*, 2019). Taken together, these observations suggest that specific TE
568 superfamily members with dynamic DNA methylation levels may contribute to stress response
569 strategies in plants.

570

571 **DMR location preferences for centromeric regions**

572 It has long been established that DNA methylation is enriched in peri-/centromeric regions which
573 follow the distribution of TEs over the chromosomes of genomes of the Brassicaceae family, as
574 recently also confirmed for *Thlaspi arvense* (Seymour *et al.*, 2014; X. Zhang *et al.*, 2006; Naish *et*
575 *al.*, 2021; Nunn *et al.*, 2022;). In our study, investigating the global distribution of DMRs over the

576 *F. vesca* chromosomes, we found that regions with high DMR density correlated with regions
577 enriched in *Helitrons*. Interestingly, we made this observation for all stress conditions (Fig. 7a, b).
578 Currently, *F. vesca* centromeres are not well defined; however, a genome-wide scan of the *F. vesca*
579 genome for tandem repeats suggested the presence of *Helitrons* near the centromeres (Xiong *et al.*
580 *et al.*, 2016). This suggests that *F. vesca* centromeres or pericentromeric regions respond to stresses
581 with DNA methylation changes. To further confirm the exact localization of *F. vesca* centromeres,
582 immunoprecipitations using a CENH3 antibody followed by sequencing will be required (Comai
583 *et al.*, 2017). Why centromere-associated regions are more prone to DNA methylation changes
584 and the physiological relevance of this observation still needs to be determined.

585

586 **Heat-stress results in loss of methylation in regions flanking TFs**

587 In our study, the global analysis of the DMRs resulting from each stress condition highlighted
588 numerous shared genomic patterns among the stresses but also interesting stress-specific genomic
589 features. In the case of heat stress, we observed hypoDMRs predominantly in gene, promoter, and
590 TE regions. Extreme temperatures are one of the main stresses affecting plants that particularly
591 alter their development and potentially cause yield loss (Janni *et al.*, 2020). Heat response triggers
592 a chain of highly conserved mechanisms (Ohama *et al.*, 2017; de Vries *et al.*, 2020; Medina *et al.*,
593 2021). In the case of *F. vesca*, we found that DNA methylation differences were enriched in genes
594 related to transcription factor regulation and activity as well as generators of metabolites and
595 energy. This result is consistent with the idea that transcription factors are required to reprogram
596 stress-related genes (Ohama *et al.*, 2016). There is evidence which showed heat stress response
597 requires not only transcription factor activity but also epigenetic regulators and small RNAs to
598 rapidly activate genes (Ohama *et al.*, 2017). However, little is known about how these responses
599 are influenced directly by changes in DNA methylation or *vice versa*. Transcription factor families
600 such as *AP2/EREBP* and *HSFs* play important roles in response to abiotic stresses in plants
601 including strawberry, apple and maize (Brown *et al.*, 2016; H. C. Liu *et al.*, 2011; Qian *et al.*,
602 2019; Xie *et al.*, 2019; C. L. Zhang *et al.*, 2020). More over, some *AP2/EREBP* genes are known
603 to be highly induced under heat stress conditions and up-regulated by HSFs through an
604 interconnected stress regulatory network (Q. Liu *et al.*, 1998; H. C. Liu *et al.*, 2011). Here, we
605 provide epigenetic evidence which suggests that members of the *AP2/EREBP* might be regulated
606 by changes in DNA methylation in *F. vesca*. Among them, the promoter region of the ethylene

607 response factor *EFR30* gene showed loss of methylation and significant up-regulation after heat
608 stress. Recent studies showed that ERFs enhance basal thermotolerance by regulating heat-
609 responsive genes and interacting with HSF in Arabidopsis and tomato (Klay et al., 2018; Huang
610 et al., 2021). Similarly, hypomethylation in the TSS of genes involved in the control of cell growth
611 in tobacco and stress-tolerance genes in maize after heat stress exposure is consistent with the
612 increase in their transcription levels (Centomani et al., 2015; Qian et al., 2019). Correspondingly,
613 we identified 58% of *HSFs* genes with hypoDMRs in their promoter regions after heat stress. *HSFs*
614 are crucial for thermotolerance capacity and regulate the expression of several heat-stress response
615 genes as Heat shock proteins (HSPs) (Liu et al., 2011). Here, we showed up-regulation of class A
616 and B *HFSs* in *F. vesca* after heat stress. Comparable results were obtained in a transcriptome
617 analysis of the octoploid strawberry where *HSF* expression was induced by a heat shock treatment
618 (Liao et al., 2016). Taken together, these findings provide insights into stress induced DNA
619 methylation as plant response, and it will be of great interest to investigate the role of DNA
620 hypomethylation in promoter regions of *AP2/EREBP* and *HSF* genes in regulating or priming
621 transcription during heat stress in *F. vesca*.

622 **Conclusions**

623 In summary, our data revealed how DNA methylation profiles at genes and transposable elements
624 can vary in response to stresses in wild strawberry. In addition, we observed correlations between
625 changes in DNA methylation and gene regulation as interconnected mechanisms during stress
626 exposure. We provide insights into how specific chromosomal regions can vary at DNA
627 methylation levels under stress conditions. These observations suggest that the epigenetic
628 flexibility of centromeres may play an important role during plant stress response. Furthermore,
629 using *F. vesca* as a model plant will help to better understand the stress response of more complex
630 genomes in the Rosacea family. Overall, this study with high-resolution methylome mapping of
631 the *F. vesca* genome will contribute to a better comprehension of epigenetic responses under
632 variable growth conditions. It remains to be tested if such epigenetic changes can be inherited
633 during sexual or clonal propagation (which is common in *F. vesca*) and if such changes could
634 contribute to adaptation to changing environments.

635 **Funding**

636 The European Training Network “EpiDiverse” received funding from the EU Horizon 2020
637 program under Marie Skłodowska-Curie grant agreement No 764965; The European Research
638 Council (ERC) under the European Union’s Horizon 2020 research and innovation program
639 [725701, BUNGEE, to E.B.]. Funding for open access charge: Agroscope institutional funding.

640 **Acknowledgements**

641 This study was supported by INRAE, Angers-Nantes, France and Agroscope, Nyon-Switzerland.
642 We would like to thank all the members of the EpiDiverse consortium (www.epidiverse.eu) and
643 the Crop Genome Dynamics research group for invaluable support, Katharina Jandrasits for
644 preparing WGBS libraries and Dr. Marta Robertson for the careful reading of the manuscript.

645 **Author Contribution**

646 ME.L and E.B conceived the study. ME.L performed the experiments, analyzed the methylome
647 data and wrote the manuscript. D.R. assembled the *F. vesca* genome and wrote the manuscript.
648 C.B. performed experiments and wrote the manuscript. B.D wrote the manuscript. E.B. designed
649 experiments, analyzed data, set up the genome browser and wrote the manuscript.

650

651 **Competing interests**

652 The authors declare they have no conflicts of interest.

653

654 **References**

- 655 **Alonso C, Pérez R, Bazaga P, Herrera CM. 2015.** Global DNA cytosine methylation as an
656 evolving trait: Phylogenetic signal and correlated evolution with genome size in angiosperms.
657 *Frontiers in Genetics* **5**: 1–9.
- 658 **Amil-Ruiz F, Garrido-Gala J, Blanco-Portales R, Folta KM, Muñoz-Blanco J, Caballero**
659 **JL. 2013.** Identification and Validation of Reference Genes for Transcript Normalization in
660 Strawberry (*Fragaria × ananassa*) Defense Responses. *PLoS ONE* **8**.
- 661 **Becker C, Hagmann J, Müller J, Koenig D, Stegle O, Borgwardt K, Weigel D. 2011.**
662 Spontaneous epigenetic variation in the *Arabidopsis thaliana* methylome. *Nature* **480**: 245–249.
- 663 **Bewick AJ, Schmitz RJ. 2017.** Gene body DNA methylation in plants. *Current opinion in plant*
664 *biology* **36**: 103–110.
- 665 **Bewick AJ, Zhang Y, Wendte JM, Zhang X, Schmitz RJ. 2019.** Evolutionary and
666 Experimental Loss of Gene Body Methylation and Its Consequence to Gene Expression.
667 *G3 & #58; Genes/Genomes/Genetics* **9**: 2441–2445.
- 668 **Bioinformatics B, Muller PY, Miserez AR, Dobbie Z. 2002.** Short Technical Report
669 Processing of Gene Expression Data Generated. *Gene Expression* **32**: 1372–1379.

- 670 **Brown R, Wang H, Dennis M, Slovin J, Turechek WW. 2016.** The Effects of Heat Treatment
671 on the Gene Expression of Several Heat Shock Protein Genes in Two Cultivars of Strawberry.
672 *International Journal of Fruit Science* **16**: 239–248.
- 673 **Bucher E, Reinders J, Mirouze M. 2012.** Epigenetic control of transposon transcription and
674 mobility in Arabidopsis. *Current Opinion in Plant Biology* **15**: 503–510.
- 675 **Centomani I, Sgobba A, D’Addabbo P, Dipierro N, Paradiso A, De Gara L, Dipierro S,**
676 **Viggiano L, de Pinto MC. 2015.** Involvement of DNA methylation in the control of cell growth
677 during heat stress in tobacco BY-2 cells. *Protoplasma* **252**: 1451–1459.
- 678 **Cheng J, Niu Q, Zhang B, Chen K, Yang R, Zhu JK, Zhang Y, Lang Z. 2018.**
679 Downregulation of RdDM during strawberry fruit ripening. *Genome Biology* **19**: 1–14.
- 680 **Colaneri AC, Jones AM. 2013.** Genome-Wide Quantitative Identification of DNA
681 Differentially Methylated Sites in Arabidopsis Seedlings Growing at Different Water Potential.
682 *PLoS ONE* **8**.
- 683 **Comai L, Maheshwari S, Marimuthu MPA. 2017.** Plant centromeres. *Current Opinion in*
684 *Plant Biology* **36**: 158–167.
- 685 **Danecek P, Bonfield JK, Liddle J, Marshall J, Ohan V, Pollard MO, Whitwham A, Keane**
686 **T, McCarthy SA, Davies RM, et al. 2021.** Twelve years of SAMtools and BCFtools.
687 *GigaScience* **10**: 1–4.
- 688 **Deniz Ö, Frost JM, Branco MR. 2019.** Regulation of transposable elements by DNA
689 modifications. *Nature Reviews Genetics*.
- 690 **van Dijk K, Ding Y, Malkaram S, Riethoven JJM, Liu R, Yang J, Laczko P, Chen H, Xia**
691 **Y, Ladunga I, et al. 2010.** Dynamic changes in genome-wide histone H3 lysine 4 methylation
692 patterns in response to dehydration stress in Arabidopsis thaliana. *BMC Plant Biology* **10**: 1–12.
- 693 **Dong C, Xi Y, Chen X, Cheng ZM. 2021.** Genome-wide identification of AP2/EREBP in
694 *Fragaria vesca* and expression pattern analysis of the FvDREB subfamily under drought stress.
695 *BMC plant biology* **21**: 295.
- 696 **Dowen RH, Pelizzola M, Schmitz RJ, Lister R, Dowen JM, Nery JR, Dixon JE, Ecker JR.**
697 **2012.** Widespread dynamic DNA methylation in response to biotic stress. *Proceedings of the*
698 *National Academy of Sciences of the United States of America* **109**.
- 699 **Dubin MJ, Zhang P, Meng D, Remigereau MS, Osborne EJ, Casale FP, Drewe P, Kahles**
700 **A, Jean G, Vilhjálmsson B, et al. 2015.** DNA methylation in Arabidopsis has a genetic basis
701 and shows evidence of local adaptation. *eLife* **4**: 1–23.
- 702 **Edger PP, Poorten TJ, VanBuren R, Hardigan MA, Colle M, McKain MR, Smith RD,**
703 **Teresi SJ, Nelson ADL, Wai CM, et al. 2019.** Origin and evolution of the octoploid strawberry
704 genome. *Nature Genetics* **51**: 541–547.
- 705 **Edger PP, VanBuren R, Colle M, Poorten TJ, Wai CM, Niederhuth CE, Alger EI, Ou S,**
706 **Acharya CB, Wang J, et al. 2018.** Single-molecule sequencing and optical mapping yields an
707 improved genome of woodland strawberry (*Fragaria vesca*) with chromosome-scale contiguity.
708 *GigaScience* **7**: 1–7.
- 709 **Fan HH, Wei J, Li TC, Li ZP, Guo N, Cai YP, Lin Y. 2013.** DNA methylation alterations of
710 upland cotton (*Gossypium hirsutum*) in response to cold stress. *Acta Physiologiae Plantarum* **35**:
711 2445–2453.
- 712 **Fedoroff N V. 2012.** Transposable elements, epigenetics, and genome evolution. *Science* **338**:
713 758–767.
- 714 **Fojtová M, Kovařík A, Matyášek R. 2001.** Cytosine methylation of plastid genome in higher
715 plants. Fact or artefact? *Plant Science* **160**: 585–593.

716 **Guarino F, Cicatelli A, Brundu G, Heinze B, Castiglione S. 2015.** Epigenetic diversity of
717 clonal white poplar (*populus alba* L.) populations: Could methylation support the success of
718 vegetative reproduction strategy? *PLoS ONE* **10**: 1–3.

719 **Healey A, Furtado A, Cooper T, Henry RJ. 2014.** Protocol: A simple method for extracting
720 next-generation sequencing quality genomic DNA from recalcitrant plant species. *Plant Methods*
721 **10**: 1–8.

722 **Hossain MS, Kawakatsu T, Kim K Do, Zhang N, Nguyen CT, Khan SM, Batek JM, Joshi**
723 **T, Schmutz J, Grimwood J, et al. 2017.** Divergent cytosine DNA methylation patterns in
724 single-cell, soybean root hairs. *New Phytologist* **214**: 808–819.

725 **Hu Y, Han YT, Wei W, Li YJ, Zhang K, Gao YR, Zhao FL, Feng JY. 2015.** Identification,
726 isolation, and expression analysis of heat shock transcription factors in the diploid woodland
727 strawberry *Fragaria Vesca*. *Frontiers in Plant Science* **6**: 1–16.

728 **Huang J, Zhao X, Bürger M, Wang Y, Chory J. 2021.** Two interacting ethylene response
729 factors regulate heat stress response. *The Plant cell* **33**: 338–357.

730 **Janni M, Gullì M, Maestri E, Marmioli M, Valliyodan B, Nguyen HT, Marmioli N, Foyer**
731 **C. 2020.** Molecular and genetic bases of heat stress responses in crop plants and breeding for
732 increased resilience and productivity. *Journal of Experimental Botany* **71**: 3780–3802.

733 **Jiang C, Mithani A, Belfield EJ, Mott R, Hurst LD, Harberd NP. 2014.** Environmentally
734 responsive genome-wide accumulation of de novo *Arabidopsis thaliana* mutations and
735 epimutations. *Genome Research* **24**: 1821–1829.

736 **Jühling F, Kretzmer H, Bernhart SH, Otto C, Stadler PF, Hoffmann S. 2016.** Metilene: Fast
737 and sensitive calling of differentially methylated regions from bisulfite sequencing data. *Genome*
738 *Research* **26**: 256–262.

739 **Jung S, Lee T, Cheng CH, Buble K, Zheng P, Yu J, Humann J, Ficklin SP, Gasic K, Scott**
740 **K, et al. 2019.** 15 years of GDR: New data and functionality in the Genome Database for
741 Rosaceae. *Nucleic Acids Research* **47**: D1137–D1145.

742 **Kawakatsu T, Huang S shan C, Jupe F, Sasaki E, Schmitz RJJ, Urich MAA, Castanon R,**
743 **Nery JRR, Barragan C, He Y, et al. 2016.** Epigenomic Diversity in a Global Collection of
744 *Arabidopsis thaliana* Accessions. *Cell* **166**: 492–505.

745 **Kenchanmane Raju SK, Ritter EJ, Niederhuth CE. 2019.** Establishment, maintenance, and
746 biological roles of non-CG methylation in plants. *Essays in Biochemistry* **63**: 743–755.

747 **Kersey PJ. 2019.** Plant genome sequences: past, present, future. *Current Opinion in Plant*
748 *Biology* **48**: 1–8.

749 **Klay I, Gouia S, Liu M, Mila I, Khoudi H, Bernadac A, Bouzayen M, Pirrello J. 2018.**
750 Ethylene Response Factors (ERF) are differentially regulated by different abiotic stress types in
751 tomato plants. *Plant Science* **274**: 137–145.

752 **De Kort H, Panis B, Deforce D, Van Nieuwerburgh F, Honnay O. 2020.** Ecological
753 divergence of wild strawberry DNA methylation patterns at distinct spatial scales. *Molecular*
754 *Ecology* **29**: 4871–4881.

755 **Kort H De, Toivainen T, Nieuwerburgh F Van, Panis B, Hytönen TP, Honnay O. 2021.**
756 Standing covariation between genomic and epigenomic patterns as source for natural selection in
757 wild strawberry plants. *bioRxiv*: 2021.03.31.437859.

758 **Kou HP, Li Y, Song XX, Ou XF, Xing SC, Ma J, Von Wettstein D, Liu B. 2011.** Heritable
759 alteration in DNA methylation induced by nitrogen-deficiency stress accompanies enhanced
760 tolerance by progenies to the stress in rice (*Oryza sativa* L.). *Journal of Plant Physiology* **168**:
761 1685–1693.

- 762 **Kuhlmann M, Finke A, Mascher M, Mette MF. 2014.** DNA methylation maintenance
763 consolidates RNA-directed DNA methylation and transcriptional gene silencing over generations
764 in *Arabidopsis thaliana*. *Plant Journal* **80**: 269–281.
- 765 **Lämke J, Bäurle I. 2017.** Epigenetic and chromatin-based mechanisms in environmental stress
766 adaptation and stress memory in plants. *Genome Biology* **18**: 1–11.
- 767 **Law JA, Jacobsen SE. 2010.** Establishing, maintaining and modifying DNA methylation
768 patterns in plants and animals. *Nature Reviews Genetics* **11**: 204–220.
- 769 **Li H. 2018.** Minimap2: Pairwise alignment for nucleotide sequences. *Bioinformatics* **34**: 3094–
770 3100.
- 771 **Li A, Chen L, Liu Z, Cui M, Shangguan L, Jia H, Fang J. 2018.** Characterization of
772 strawberry (*Fragaria vesca*) sequence genome. *bioRxiv*.
- 773 **Li H, Handsaker B, Wysoker A, Fennell T, Ruan J, Homer N, Marth G, Abecasis G,
774 Durbin R. 2009.** The Sequence Alignment/Map format and SAMtools. *Bioinformatics* **25**:
775 2078–2079.
- 776 **Li R, Hu F, Li B, Zhang Y, Chen M, Fan T, Wang T. 2020.** Whole genome bisulfite
777 sequencing methylome analysis of mulberry (*Morus alba*) reveals epigenome modifications in
778 response to drought stress. *Scientific Reports* **10**: 1–17.
- 779 **Li Y, Pi M, Gao Q, Liu Z, Kang C. 2019.** Updated annotation of the wild strawberry *Fragaria*
780 *vesca* V4 genome. *Horticulture Research* **6**.
- 781 **Liao WY, Lin LF, Jheng JL, Wang CC, Yang JH, Chou ML. 2016.** Identification of heat
782 shock transcription factor genes involved in thermotolerance of octoploid cultivated strawberry.
783 *International Journal of Molecular Sciences* **17**: 1–21.
- 784 **Liu Q, Kasuga M, Sakuma Y, Abe H, Miura S. 1998.** Domain Separate Two Cellular Signal
785 Transduction Pathways in Drought-and Low-Temperature. *The Plant Cell Online* **10**: 1391–
786 1406.
- 787 **Liu HC, Liao HT, Charng YY. 2011.** The role of class A1 heat shock factors (HSFA1s) in
788 response to heat and other stresses in *Arabidopsis*. *Plant, Cell and Environment* **34**: 738–751.
- 789 **Lu C, Chen J, Zhang Y, Hu Q, Su W, Kuang H. 2012.** Miniature inverted-repeat transposable
790 elements (MITEs) have been accumulated through amplification bursts and play important roles
791 in gene expression and species diversity in *oryza sativa*. *Molecular Biology and Evolution* **29**:
792 1005–1017.
- 793 **MacKelprang R, Lemaux PG. 2020.** Genetic Engineering and Editing of Plants: An Analysis
794 of New and Persisting Questions. *Annual Review of Plant Biology* **71**: 659–687.
- 795 **Mao H, Wang H, Liu S, Li Z, Yang X, Yan J, Li J, Tran LSP, Qin F. 2015.** A transposable
796 element in a NAC gene is associated with drought tolerance in maize seedlings. *Nature*
797 *Communications* **6**: 1–7.
- 798 **Matzke MA, Mosher RA. 2014.** RNA-directed DNA methylation: An epigenetic pathway of
799 increasing complexity. *Nature Reviews Genetics* **15**: 394–408.
- 800 **Medina E, Kim SH, Yun M, Choi WG. 2021.** Recapitulation of the function and role of *ros*
801 generated in response to heat stress in plants. *Plants* **10**: 1–13.
- 802 **Naish M, Alonge M, Wlodzimierz P, Tock AJ, Abramson BW, Schmücker A, Mandáková
803 T, Jamge B, Lambing C, Kuo P, et al. 2021.** The genetic and epigenetic landscape of the
804 *Arabidopsis* centromeres. *Science* **374**.
- 805 **Naito K, Zhang F, Tsukiyama T, Saito H, Hancock CN, Richardson AO, Okumoto Y,
806 Tanisaka T, Wessler SR. 2009.** Unexpected consequences of a sudden and massive transposon
807 amplification on rice gene expression. *Nature* **461**: 1130–1134.

- 808 **Nguyen K Le, Grondin A, Courtois B, Gantet P. 2019.** Next-Generation Sequencing
809 Accelerates Crop Gene Discovery. *Trends in Plant Science* **24**: 263–274.
- 810 **Niederhuth CE, Bewick AJ, Ji L, Alabady MS, Kim K Do, Li Q, Rohr NA, Rambani A,**
811 **Burke JM, Udall JA, et al. 2016.** Widespread natural variation of DNA methylation within
812 angiosperms. *Genome Biology* **17**: 1–19.
- 813 **Noshay JM, Anderson SN, Zhou P, Ji L, Ricci W, Lu Z, Stitzer MC, Crisp PA, Hirsch CN,**
814 **Zhang X, et al. 2019.** Monitoring the interplay between transposable element families and DNA
815 methylation in maize. *PLoS Genetics* **15**: 1–25.
- 816 **Nunn A, Can SN, Otto C, Fasold M, Stadler PF, Langenberger D. 2021a.** EpiDiverse
817 Toolkit : a pipeline suite for the analysis of bisulfite sequencing data in ecological plant
818 epigenetics. **3**: 1–7.
- 819 **Nunn A, Otto C, Stadler PF, Langenberger D. 2021b.** Comprehensive benchmarking of
820 software for mapping whole genome bisulfite data: from read alignment to DNA methylation
821 analysis. *Briefings in Bioinformatics* **00**: 1–9.
- 822 **Nunn A, Rodríguez-Arévalo I, Tandukar Z, Frels K, Contreras-Garrido A, Carbonell-**
823 **Bejerano P, Zhang P, Ramos Cruz D, Jandrasits K, Lanz C, et al. 2022.** Chromosome-level
824 *Thlaspi arvense* genome provides new tools for translational research and for a newly
825 domesticated cash cover crop of the cooler climates . *Plant Biotechnology Journal*: 1–20.
- 826 **Ohama N, Kusakabe K, Mizoi J, Zhao H, Kidokoro S, Koizumi S, Takahashi F, Ishida T,**
827 **Yanagisawa S, Shinozaki K, et al. 2016.** The transcriptional cascade in the heat stress response
828 of *Arabidopsis* is strictly regulated at the level of transcription factor expression. *Plant Cell* **28**:
829 181–201.
- 830 **Ohama N, Sato H, Shinozaki K, Yamaguchi-Shinozaki K. 2017.** Transcriptional Regulatory
831 Network of Plant Heat Stress Response. *Trends in Plant Science* **22**: 53–65.
- 832 **Omidvar V, Fellner M. 2015.** DNA methylation and transcriptomic changes in response to
833 different lights and stresses in 7B-1 male-sterile tomato. *PLoS ONE* **10**: 1–23.
- 834 **Ou S, Su W, Liao Y, Chougule K, Agda JRA, Hellings AJ, Lugo CSB, Elliott TA, Ware D,**
835 **Peterson T, et al. 2019.** Benchmarking transposable element annotation methods for creation of
836 a streamlined, comprehensive pipeline. *Genome Biology* **20**: 1–18.
- 837 **Ou X, Zhang Y, Xu C, Lin X, Zang Q, Zhuang T, Jiang L, von Wettstein D, Liu B. 2012.**
838 Transgenerational Inheritance of Modified DNA Methylation Patterns and Enhanced Tolerance
839 Induced by Heavy Metal Stress in Rice (*Oryza sativa* L.). *PLoS ONE* **7**.
- 840 **Pan Y, Wang W, Zhao X, Zhu L, Fu B, Li Z. 2011.** DNA methylation alterations of rice in
841 response to cold stress. *Plant OMICS* **4**: 364–369.
- 842 **Pedersen BS, Quinlan AR. 2018.** Mosdepth: Quick coverage calculation for genomes and
843 exomes. *Bioinformatics* **34**: 867–868.
- 844 **Prezza N, Del Fabbro C, Vezzi F, De Paoli E, Policriti A. 2012.** ERNE-BS5: Aligning BS-
845 treated sequences by multiple hits on a 5-letters alphabet. *2012 ACM Conference on*
846 *Bioinformatics, Computational Biology and Biomedicine, BCB 2012*: 12–19.
- 847 **Qian Y, Hu W, Liao J, Zhang J, Ren Q. 2019.** The Dynamics of DNA methylation in the
848 maize (*Zea mays* L.) inbred line B73 response to heat stress at the seedling stage. *Biochemical*
849 *and Biophysical Research Communications* **512**: 742–749.
- 850 **Quadrana L, Colot V. 2016.** Plant Transgenerational Epigenetics. *Annual Review of Genetics*
851 **50**: 467–491.
- 852 **Rakei A, Maali-Amiri R, Zeinali H, Ranjbar M. 2016.** DNA methylation and physio-
853 biochemical analysis of chickpea in response to cold stress. *Protoplasma* **253**: 61–76.

- 854 **Ramírez F, DüNDAR F, Diehl S, Grüning BA, Manke T. 2014.** DeepTools: A flexible platform
855 for exploring deep-sequencing data. *Nucleic Acids Research* **42**: 187–191.
- 856 **Rendina González AP, Preite V, Verhoeven KJF, Latzel V. 2018.** Transgenerational effects
857 and epigenetic memory in the clonal plant *trifolium repens*. *Frontiers in Plant Science* **871**: 1–
858 11.
- 859 **Sahu PP, Pandey G, Sharma N, Puranik S, Muthamilarasan M, Prasad M. 2013.** Epigenetic
860 mechanisms of plant stress responses and adaptation. *Plant Cell Reports* **32**: 1151–1159.
- 861 **Sammarco I, Münzbergová Z, Latzel V. 2022.** DNA Methylation Can Mediate Local
862 Adaptation and Response to Climate Change in the Clonal Plant *Fragaria vesca* : Evidence From
863 a European-Scale Reciprocal Transplant Experiment. **13**.
- 864 **Schmitz RJ, Schultz MD, Lewsey MG, O'Malley RC, Urich MA, Libiger O, Schork NJ,
865 Ecker JR. 2011.** Transgenerational epigenetic instability is a source of novel methylation
866 variants. *Science* **334**: 369–373.
- 867 **Secco D, Wang C, Shou H, Schultz MD, Chiarenza S, Nussaume L, Ecker JR, Whelan J,
868 Lister R. 2015.** Stress induced gene expression drives transient DNA methylation changes at
869 adjacent repetitive elements. *eLife* **4**: 1–26.
- 870 **Sedlazeck FJ, Rescheneder P, Smolka M, Fang H, Nattestad M, Von Haeseler A, Schatz
871 MC. 2018.** Accurate detection of complex structural variations using single-molecule
872 sequencing. *Nature Methods* **15**: 461–468.
- 873 **Seymour DK, Koenig D, Haggmann J, Becker C, Weigel D. 2014.** Evolution of DNA
874 Methylation Patterns in the Brassicaceae is Driven by Differences in Genome Organization.
875 *PLoS Genetics* **10**.
- 876 **Shan X, Wang X, Yang G, Wu Y, Su S, Li S, Liu H, Yuan Y. 2013.** Analysis of the DNA
877 methylation of maize (*Zea mays* L.) in response to cold stress based on methylation-sensitive
878 amplified polymorphisms. *Journal of Plant Biology* **56**: 32–38.
- 879 **Shen X, De Jonge J, Forsberg SKG, Pettersson ME, Sheng Z, Hennig L, Carlborg Ö. 2014.**
880 Natural CMT2 Variation Is Associated With Genome-Wide Methylation Changes and
881 Temperature Seasonality. *PLoS Genetics* **10**.
- 882 **Shulaev V, Sargent DJ, Crowhurst RN, Mockler TC, Folkerts O, Delcher AL, Jaiswal P,
883 Mockaitis K, Liston A, Mane SP, et al. 2011.** The genome of woodland strawberry (*Fragaria*
884 *vesca*). *Nature Genetics* **43**: 109–116.
- 885 **Shumate A, Salzberg SL. 2021.** Liftoff: Accurate mapping of gene annotations. *Bioinformatics*
886 **37**: 1639–1643.
- 887 **Slotkin RK, Martienssen R. 2007.** Transposable elements and the epigenetic regulation of the
888 genome. *Nature Reviews Genetics* **8**: 272–285.
- 889 **Suriyasak C, Hatanaka K, Tanaka H, Okumura T, Yamashita D, Attri P, Koga K,
890 Shiratani M, Hamaoka N, Ishibashi Y. 2021.** Alterations of DNA Methylation Caused by
891 Cold Plasma Treatment Restore Delayed Germination of Heat-Stressed Rice (*Oryza sativa* L.)
892 Seeds . *ACS Agricultural Science & Technology* **1**: 5–10.
- 893 **Tian T, Liu Y, Yan H, You Q, Yi X, Du Z, Xu W, Su Z. 2017.** AgriGO v2.0: A GO analysis
894 toolkit for the agricultural community, 2017 update. *Nucleic Acids Research* **45**: W122–W129.
- 895 **Urrutia M, Bonet J, Arús P, Monfort A. 2015.** A near-isogenic line (NIL) collection in diploid
896 strawberry and its use in the genetic analysis of morphologic, phenotypic and nutritional
897 characters. *Theoretical and Applied Genetics* **128**: 1261–1275.
- 898 **Varotto S, Tani E, Abraham E, Abraham T, Kapazoglou A, Melzer R, Radanoviæ A,
899 Miladinoviæ D. 2020.** Epigenetics: Possible applications in climate-smart crop breeding.

- 900 *Journal of Experimental Botany* **71**: 5223–5236.
- 901 **Verhoeven KJF, Jansen JJ, van Dijk PJ, Biere A. 2010.** Stress-induced DNA methylation
902 changes and their heritability in asexual dandelions. *New Phytologist* **185**: 1108–1118.
- 903 **Verhoeven KJF, VonHoldt BM, Sork VL. 2016.** Epigenetics in ecology and evolution: What
904 we know and what we need to know. *Molecular Ecology* **25**: 1631–1638.
- 905 **Vidalis A, Živković D, Wardenaar R, Roquis D, Tellier A, Johannes F. 2016.** Methylome
906 evolution in plants. *Genome Biology* **17**: 1–14.
- 907 **Vitte C, Fustier MA, Alix K, Tenailon MI. 2014.** The bright side of transposons in crop
908 evolution. *Briefings in Functional Genomics and Proteomics* **13**: 276–295.
- 909 **de Vries J, de Vries S, Curtis BA, Zhou H, Penny S, Feussner K, Pinto DM, Steinert M,
910 Cohen AM, von Schwartzberg K, et al. 2020.** Heat stress response in the closest algal
911 relatives of land plants reveals conserved stress signaling circuits. *Plant Journal* **103**: 1025–
912 1048.
- 913 **Wang P, Zhao FJ, Kopittke PM. 2019.** Engineering Crops without Genome Integration Using
914 Nanotechnology. *Trends in Plant Science* **24**: 574–577.
- 915 **Wei L, Gu L, Song X, Cui X, Lu Z, Zhou M, Wang L, Hu F, Zhai J, Meyers BC, et al. 2014.**
916 Dicer-like 3 produces transposable element-associated 24-nt siRNAs that control agricultural
917 traits in rice. *Proceedings of the National Academy of Sciences of the United States of America*
918 **111**: 3877–3882.
- 919 **Wibowo A, Becker C, Marconi G, Durr J, Price J, Hagemann J, Papareddy R, Putra H,
920 Kageyama J, Becker J, et al. 2016.** Elife-13546-V2. : 1–27.
- 921 **Williams BP, Gehring M. 2017.** Stable transgenerational epigenetic inheritance requires a DNA
922 methylation-sensing circuit. *Nature Communications* **8**.
- 923 **Xie Z, Nolan TM, Jiang H, Yin Y. 2019.** AP2/ERF transcription factor regulatory networks in
924 hormone and abiotic stress responses in Arabidopsis. *Frontiers in Plant Science* **10**: 1–17.
- 925 **Xin Y, Ma B, Xiang Z, He N. 2019.** Amplification of miniature inverted-repeat transposable
926 elements and the associated impact on gene regulation and alternative splicing in mulberry
927 (*Morus notabilis*). *Mobile DNA* **10**: 1–13.
- 928 **Xiong W, Dooner HK, Du C. 2016.** Rolling-circle amplification of centromeric Helitrons in
929 plant genomes. *Plant Journal* **88**: 1038–1045.
- 930 **Xu G, Lyu J, Li Q, Liu H, Wang D, Zhang M, Springer NM, Ross-Ibarra J, Yang J. 2020.**
931 Evolutionary and functional genomics of DNA methylation in maize domestication and
932 improvement. *Nature Communications* **11**.
- 933 **Zhang H, Lang Z, Zhu J-K. 2018.** Dynamics and function of DNA methylation in plants.
934 *Nature Reviews Molecular Cell Biology* **19**: 489–506.
- 935 **Zhang CL, Wang YX, Hu X, Zhang YL, Wang GL, You CX, Li YY, Hao YJ. 2020.** An
936 apple AP2/EREBP-type transcription factor, MdWRI4, enhances plant resistance to abiotic stress
937 by increasing cuticular wax load. *Environmental and Experimental Botany* **180**: 104206.
- 938 **Zhang L, Wang Y, Zhang X, Zhang M, Han D, Qiu C, Han Z. 2012.** Dynamics of
939 phytohormone and DNA methylation patterns changes during dormancy induction in strawberry
940 (*Fragaria × ananassa* Duch.). *Plant Cell Reports* **31**: 155–165.
- 941 **Zhang X, Yazaki J, Sundaresan A, Cokus S, Chan SWL, Chen H, Henderson IR, Shinn P,
942 Pellegrini M, Jacobsen SE, et al. 2006.** Genome-wide High-Resolution Mapping and
943 Functional Analysis of DNA Methylation in Arabidopsis. *Cell* **126**: 1189–1201.
- 944 **Zhang H, Zhu J, Gong Z, Zhu JK. 2021.** Abiotic stress responses in plants. *Nature Reviews*
945 *Genetics* **0123456789**.

- 946 **Zheng X, Chen L, Li M, Lou Q, Xia H, Wang P, Li T, Liu H, Luo L. 2013.** Transgenerational
947 variations in DNA methylation induced by drought stress in two rice varieties with distinguished
948 difference to drought resistance. *PLoS ONE* **8**: 1–13.
949
- 950 **World Meteorological Organization (WMO). State of the Global Climate 2021:** WMO
951 Provisional report. Web page:
952 https://library.wmo.int/index.php?lvl=notice_display&id=21982
953 **World Meteorological Organization (WMO). State of the Global Climate 2020** (WMO-No.
954 1264). Web page: https://library.wmo.int/index.php?lvl=notice_display&id=21880
955 **Wick R. 2017. Filtlong.** Web page :<https://github.com/rrwick/Filtlong>.
956 **“Picard Toolkit.” 2019.** Broad Institute, GitHub Repository. Web page :
957 <https://broadinstitute.github.io/picard/>
958 **Van der Auwera GA & O'Connor BD. (2020).** Genomics in the Cloud: Using Docker, GATK,
959 and WDL in Terra (1st Edition). O'Reilly Media.
960